

14 Dec 53

T1-2860

WADC TECHNICAL REPORT 52-128  
PART 1

DO NOT DESTROY  
RETURN TO  
TECHNICAL DOCUMENT  
CONTROL SECTION  
~~TT0000~~  
ASAPRL

UUI

AD A075881

**AN EXPERIMENTAL INVESTIGATION OF THE USE OF HOT  
GAS EJECTORS FOR BOUNDARY LAYER REMOVAL**

**RICHARD V. DELEO  
RICHARD D. WOOD**

**ROSEMOUNT AERONAUTICAL LABORATORIES**

**APRIL 1952**

**WRIGHT AIR DEVELOPMENT CENTER**

20011010199

## NOTICES

When Government drawings, specifications, or other data are used for any purpose other than in connection with a definitely related Government procurement operation, the United States Government thereby incurs no responsibility nor any obligation whatsoever; and the fact that the Government may have formulated, furnished, or in any way supplied the said drawings, specifications, or other data, is not to be regarded by implication or otherwise as in any manner licensing the holder or any other person or corporation, or conveying any rights or permission to manufacture, use, or sell any patented invention that may in any way be related thereto.

The information furnished herewith is made available for study upon the understanding that the Government's proprietary interests in and relating thereto shall not be impaired. It is desired that the Judge Advocate (WCJ), Wright Air Development Center, Wright-Patterson Air Force Base, Ohio, be promptly notified of any apparent conflict between the Government's proprietary interests and those of others.



WADC TECHNICAL REPORT 52-128  
PART 1

**AN EXPERIMENTAL INVESTIGATION OF THE USE OF HOT  
GAS EJECTORS FOR BOUNDARY LAYER REMOVAL**

*Richard V. DeLeo  
Richard D. Wood*

*Rosemount Aeronautical Laboratories*

*April 1952*

*Aircraft Laboratory  
Contract No. AF 33(038)-5131  
RDO No. 458-433*

Wright Air Development Center  
Air Research and Development Command  
United States Air Force  
Wright-Patterson Air Force Base, Ohio

## FOREWORD

This report was prepared by the Department of Aeronautical Engineering of the University of Minnesota under the direction of Professor John D. Akerman, Head of the Department of Aeronautical Engineering and Mr. J. Leonard Frame, Administrative Scientist at the Rosemount Aeronautical Laboratories. Research was conducted under Contract No. AF 33(038)-5131. The project was identified by Research and Development Order No. 458-433, "Boundary Layer Control," and was administered by the Aircraft Laboratory, Directorate of Laboratories, Wright Air Development Center, with Mr. Joseph J. Flatt acting as project engineer.

Technical direction of the program was under Mr. Richard V. DeLeo, Project Scientist. Dr. Rudolf Hermann was a consultant. Included among those who participated in the study were Messrs. Richard D. Wood, Joseph A. Huerta, Roland Daugherty, and Ole Flack of the Rosemount Aeronautical Laboratories.

## A B S T R A C T

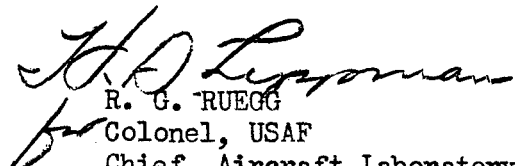
The feasibility of using an ejector with heated primary flow as a suction pump for boundary layer air removal from an aircraft has been investigated. Effects of some of the basic ejector geometric and state parameters were evaluated.

The results indicate that while boundary layer removal by this method is feasible the aerodynamic benefits so obtained are accompanied by a measurable loss of primary jet thrust. Tests show the ejector to be relatively insensitive to the geometric parameters of primary nozzle location and mixing section length. Ejector performance for a given geometry was found to be a function of the primary momentum. The addition of a diffuser substantially increased ejector performance but was accompanied by greatly reduced thrust. Results indicate that an optimum geometry exists for each combination of flow conditions.

## P U B L I C A T I O N R E V I E W

This report has been reviewed and is approved.

FOR THE COMMANDER:

  
R. G. RUEGG  
Colonel, USAF  
Chief, Aircraft Laboratory  
Directorate of Laboratories

## T A B L E O F C O N T E N T S

	<u>PAGE</u>
I. Introduction	1
A. Scope	2
II. Description of Apparatus	2
III. Test Program and Results	4
A. Bare Engine Thrust and Mass Flow	4
B. Primary Nozzle Location	4
C. Mixing Section Length and Area Ratio	6
1. Mixing Section Length	6
2. Area Ratio	7
3. Thrust Performance	8
D. Primary Temperature and Pressure	9
1. Constant Primary Pressure	9
2. Constant Primary Temperature	10
3. Constant Primary Mass Flow	11
E. Performance with Diffuser	12
F. Pressure Distribution Along Mixing Tube	14
IV. Conclusions	16
References	20

### APPENDIX

A. Nomenclature	21
B. Derivation of Momentum Relation	23
C. Derivation of Exit Mach Number Equation	24
D. Ejector Thrust as Predicted by the Momentum Equation	25
E. Application of Ejector Data to an Aircraft Installation	27

## LIST OF FIGURES

<u>FIGURE NUMBER</u>		<u>PAGE</u>
<u>General</u>		
1. Diagram:	Schematic Diagram of Ejector Application to Turbo-Jet Aircraft for Boundary Layer Air Removal.	29
2. Diagram:	Schematic Diagram of Hot Gas Ejector Installation.	30
3. Photograph:	Front View of Apparatus.	31
4. Photograph:	Rear View of Test Facility.	31
5. Photograph:	Close-Up of Bare Plenum Chamber.	32
6. Photograph:	Instruments and Control Room.	32
7. Curve:	Thrust and Primary Mass Flow versus Primary Pressure Ratio.	33
<u>Primary Nozzle Location</u>		
8. Curve:	Mass Flow Ratio versus Secondary Pressure Ratio for $A_3/A_1 = 1.72$ .	34
9. Curve:	Mass Flow Ratio versus Secondary Pressure Ratio for $A_3/A_1 = 2.48$	34
10. Curve:	Mass Flow Ratio versus Secondary Pressure Ratio for $A_3/A_1 = 4.30$ .	34
<u>Ejector Performance at Various Mixing Section Lengths</u>		
11. Curve:	Mass Flow Ratio versus Secondary Pressure Ratio for $A_3/A_1 = 1.72$ .	35
12. Curve:	Mass Flow Ratio versus Secondary Pressure Ratio for $A_3/A_1 = 2.48$ .	35
13. Curve:	Mass Flow Ratio versus Secondary Pressure Ratio for $A_3/A_1 = 4.30$ .	35
<u>Optimum Mixing Section Length</u>		
14. Curve:	Mass Flow Ratio versus Mixing Tube Length at $P_2/P_a = 0.75$ .	36
15. Curve:	Pressure Ratio versus Mixing Tube Length at $W_2/W_1 = 0.25$ .	36

FIGURE NUMBERPAGEOptimum Area Ratio

16. Curve: Mass Flow Ratio versus Area Ratio at  
 $P_2/P_a = 0.75$ . 37
17. Curve: Pressure Ratio versus Area Ratio at  
 $W_2/W_1 = 0.25$ . 37

Predicted Ejector Performance

18. Curve: Mass Flow Ratio versus Area Ratio. 38

Ejector Thrust for Various Mixing Section Lengths

19. Curve: Thrust versus Secondary Pressure Ratio  
for  $A_3/A_1 = 1.72$ . 39
20. Curve: Thrust versus Secondary Pressure Ratio  
for  $A_3/A_1 = 2.48$ . 39
21. Curve: Thrust versus Secondary Pressure Ratio  
for  $A_3/A_1 = 4.30$ . 39

Performance at Constant Primary Pressure

22. Curve: Mass Flow Ratio versus Secondary Pressure  
Ratio for  $P_1/P_a = 1.91$ . 40
23. Curve: Thrust versus Secondary Pressure Ratio  
for  $P_1/P_a = 1.91$ . 40

Performance at Constant Primary Temperature

24. Curve: Mass Flow Ratio versus Secondary Pressure  
Ratio for  $T_1 = 1200^\circ\text{F}$ . 41
25. Curve: Thrust versus Secondary Pressure Ratio  
for  $T_1 = 1200^\circ\text{F}$ . 41

Performance at Constant Primary Mass Flow

26. Curve: Mass Flow Ratio versus Secondary Pressure  
Ratio at  $W_1 = 4.81 \text{ \#/sec}$ . 42
27. Curve: Thrust versus Secondary Pressure Ratio  
at  $W_1 = 4.81 \text{ \#/sec}$ . 42

FIGURE NUMBERPAGEOptimum Primary Pressure Ratio

28. Curves: Secondary Pressure Ratio versus Primary Pressure Ratio at Various Mass Flow Ratios. 43

Ejector Performance with Diffuser

29. Curve: Mass Flow Ratio versus Secondary Pressure Ratio for  $A_3/A_1 = 1.72$ . 44
30. Curve: Mass Flow Ratio versus Secondary Pressure Ratio for  $A_3/A_1 = 2.48$ . 44
31. Curve: Mass Flow Ratio versus Secondary Pressure Ratio for  $A_3/A_1 = 4.30$ . 44
32. Curve: Mass Flow Ratio versus Secondary Pressure Ratio (at different mixing tube lengths) 45

Pressure Distribution Along Mixing Tube

33. Curve: Static Pressure Ratio versus Distance Along Mixing Tube for  $A_3/A_1 = 1.72$  at  $W_2/W_1 = 0$ . 46
34. Curve: Static Pressure Ratio versus Distance Along Mixing Tube for  $A_3/A_1 = 1.72$  at  $W_2/W_1 = 0.15$ . 46
35. Curve: Static Pressure Ratio versus Distance Along Mixing Tube for  $A_3/A_1 = 1.72$  at  $W_2/W_1 = 0.30$ . 46
36. Curve: Static Pressure Ratio versus Distance Along Mixing Tube for  $A_3/A_1 = 2.48$  at  $W_2/W_1 = 0$ . 47
37. Curve: Static Pressure Ratio versus Distance Along Mixing Tube for  $A_3/A_1 = 2.48$  at  $W_2/W_1 = 0.20$ . 47
38. Curve: Static Pressure Ratio versus Distance Along Mixing Tube for  $A_3/A_1 = 2.48$  at  $W_2/W_1 = 0.40$ . 47
39. Curve: Static Pressure Ratio versus Distance Along Mixing Tube for  $A_3/A_1 = 4.30$  at  $W_2/W_1 = 0, 0.20, 0.40$ . 48
40. Curve: Static Pressure Ratio versus Distance Along Mixing Tube for  $A_3/A_1 = 1.72$  at  $W_2/W_1 = 0$  for Different Mixing Tube Lengths. 49
41. Curve: Static Pressure Ratio versus Distance Along Mixing Tube for  $A_3/A_1 = 1.72$  at  $W_2/W_1 = 0.15$  for Different Mixing Tube Lengths. 49



## I. INTRODUCTION

The problem of controlling the boundary layer formed on the surface of the wing of an airplane is becoming increasingly important as the speed of present day aircraft approaches sonic velocity. At high speeds the drag caused by separation of the flow behind local shock waves creates a serious loss in performance. The problem of maintaining adequate aileron control with forward separation at high speeds is an especially serious one. In low speed flight premature separation of the flow occurs at high angles of attack which limits the maximum coefficient of lift as well as causing a large increase in drag.

A previous investigation, Air Force Technical Report Number 6344, Investigation of Boundary Layer Control at High Speeds, by this department indicates that the desirable boundary layer control can be obtained by means of suction through thin spanwise slots or a porous surface normal to the direction of the airflow on the top surface of the wing. The over-all economy, in terms of reduction in drag and effect on lift, of this method of boundary layer control depends not only on the net improvement in performance, but on the necessary value of the suction coefficient at which this maximum performance takes place.

A major problem in the use of such a system is that of obtaining a power or suction source large enough but still simple, light, compact, and dependable. It was felt that the inductive action of an ejector using the exhaust gases of a turbo-jet would offer a large potential power source for use in the removal of boundary layer air.

Preliminary study indicated that it was both practical and feasible to use such an ejector system as a source of boundary layer suction although little experimental work had been done on the subject. A schematic diagram of a possible ejector arrangement applied to turbo-jet aircraft is shown in Figure 1.

#### A. Scope

The objective of this project was to conduct an experimental and analytical study of ejectors using a hot gas exhaust for primary flow for use as a means of pumping the air necessary for boundary layer control. The basic geometric parameters and operating conditions of the ejector and its location with respect to the primary jet, over a range consistent with the size and performance requirements of modern aircraft, were investigated.

Operating conditions of the primary hot gas flow were held constant for the majority of the tests since it was felt that a sufficient indication of ejector performance would be given with a great saving in the number of test runs required.

As a final part of the test program a diffuser was added to each of several mixing tube configurations. It was realized that the addition of a diffuser would yield a higher performance ejector configuration with essentially zero net thrust. Such a configuration could be used for boundary layer removal in a reciprocating engine installation where the exhaust thrust is unimportant and the mass flow of the hot primary gas is very limited.

## II. DESCRIPTION OF APPARATUS

A schematic drawing of the test installation is shown in Figure 2 with photographs of the apparatus in Figures 3, 4, 5 and 6.

The basic unit is the TG-180 combustion chamber which was used as a source of high temperature exhaust gases. The entire test set-up was designed around this unit. Equipped with the conventional spray fuel

nozzle and spark ignition system the combustion chamber is mounted with a convergent exhaust nozzle to obtain a sonic primary jet.

Around the exhaust jet and the end of the combustion chamber is mounted a large chamber constructed from a section of a 20-inch diameter steel pipe. The chamber is sealed around the burner on one end and is open on the other. It is used both as a plenum chamber for the induced secondary air and as a mount for the entrance cone and mixing tube of the ejector system. Black iron pipe was used for the mixing tubes and the cones were fabricated from #10 gauge sheet steel.

The entire ejector system (cone and mixing tube) was adjustable horizontally to allow for determination of the optimum primary nozzle location. The cone was sealed to the plenum chamber for each test by a special, removable, rubber compression gasket to insure an accurate determination of secondary operation conditions.

The entire set-up (combustion chamber, plenum chamber, and ejector system) is mounted on a free riding thrust table. This table was allowed to act against a small cantilever beam fastened to a stationary frame. Two strain gages, one glued to each side of the beam, were connected into a wheatstone bridge circuit and pressure against the beam caused an unbalance in the circuit which deflected the galvanometer. This deflection of the galvanometer was calibrated to read pounds of thrust.

A simple 7 degree conical diffuser was constructed from #10 gauge sheet steel. Built in three sections to enable its use with any of three different diameter mixing tubes it was fastened by means of flanges to the exit of the mixing tube.

The primary air was obtained from a reciprocating compressor delivering a mass flow of approximately 4.5 pounds per second. Induced or secondary air was taken from the atmosphere. Each source of air was controlled by a separate valve, and the actual mass of air was measured by an orifice plate. A butterfly valve using a hydraulic actuator control was used on the secondary air line.

Kerosene was used for fuel and was controlled by means of a needle valve. Both a temperature cut-off and mercury pressure switch were

connected in the fuel line as safety devices. Spark ignition for the combustion chamber was obtained from a 12,000 volt transformer.

All temperatures were read by means of thermocouples connected to a 24-channel Brown 0° to 2000°F potentiometer. The various primary and secondary air pressures were read both from Bourdon gages and Meriam differential manometers. Standard U tubes were used for all orifice and static pressure measurements.

### III. TEST PROGRAM AND RESULTS

Early in the test program a schedule of tests to be made was determined. It was decided to divide the test program into five separate sections. Completion and interpretation of the results of each section was required before proceeding to the next test.

#### A. Bare Engine Thrust and Mass Flow

The initial test was a determination and verification of the thrust and mass flow of the primary heated jet system. The entire ejector system was omitted during these tests. Thrust and mass flow measurements were made at five primary pressure ratios ranging from,  $P_1/P_a = 1.25$  to 2.0, while holding the primary stagnation temperature constant at  $T_1 = 1200^\circ\text{F}$ . The strain gages attached to the cantilever beam were carefully calibrated and gave an accurate measurement of the thrust at all pressure ratios. Primary mass flow readings were obtained from an orifice plate upstream of the unit in the supply piping. Experimental results were compared with theoretical values calculated for the same conditions. Both theoretical and experimental values of thrust and mass flow are plotted in Figure 7. Good agreement between the actual and theoretical values of mass flow and thrust was obtained with the maximum difference being less than 4 per cent.

#### B. Primary Nozzle Location

The effect of primary nozzle location upon ejector performance was evaluated at three diameters of mixing tubes. Nominal diameters tested were 5, 6, and 8 inches with the primary jet diameter fixed at 3.86 inches. The primary nozzle was fixed in location but the mixing tube and entrance cone were movable. Each could be adjusted fore and aft by means of

external adjusting screws to move the mixing entrance cone with respect to the fixed plenum chamber and primary nozzle.

A realistic primary air temperature and total pressure within the normal operating range of a modern turbo-jet is  $T_1/T_a = 3.32$  and  $P_1/P_a = 1.91$ . The above conditions insure sonic Mach number at the exit of the exhaust nozzle which is typical of present day operations. Operating the primary nozzle at the above conditions, tests were made with the primary nozzle at five different axial positions. The position of the jet with respect to the entrance of the mixing tube was varied from one mixing tube diameter ( $D_3$ ) upstream of the entrance to one diameter downstream or with the primary nozzle actually inserted into the mixing tube. The exact positions were: primary nozzle position ( $Q$ ) =  $\pm D_3$ ;  $\pm 1/2 D_3$ ; and  $0 D_3$ .

As can be seen from Figure 2, a change in primary nozzle position ( $Q$ ) also varies the effective mixing section length ( $L$ ). To minimize this effect, all tests were conducted with a mixing tube length of ten diameters. Therefore, the movement of the primary jet had only a small percentage effect on the overall mixing tube length. Tests run later in the program showed that the above variable could be neglected at mixing tube lengths ( $L$ ) between 7 and  $10 D_3$ .

Testing results showing the effect of primary nozzle location on ejector performance are presented in Figures 8, 9 and 10. Five test values of mass flow ratio ( $W_2/W_1$ ) and thrust were obtained for each nozzle location by adjusting the secondary throttling valve between the limits of maximum and minimum secondary pressures. The secondary orifice manometers were read at each point and the secondary mass flow calculated.

The testing results show that the ejector is relatively insensitive to nozzle position between the limits of ( $Q$ ) =  $+ D_3$  to  $-1/2 D_3$ . Performance definitely drops off when the primary nozzle is more than one half of a mixing tube diameter ( $D_3$ ) upstream of the entrance to the tube or at ( $Q$ ) =  $D_3$  for both the 5-inch and 6-inch mixing tubes, or at  $(A_3/A_1) = 1.72$  and  $2.48$ . Testing results for the 8-inch mixing tube,  $(A_3/A_1) = 4.30$ , show that variation of the primary nozzle position had no appreciable effect upon the performance within the range tested.

An attempt was made to test the effect of primary nozzle location with a 4-inch mixing tube, but it was found that no vacuum or secondary mass flow was produced, so this configuration was not tested further. Apparently, the mixing tube to primary nozzle area ratio of  $(A_3/A_1) = 1.09$  was not sufficient to allow the induction of a secondary mass flow, in fact, it was noted that a slight back pressure was built up in the secondary line. Evidently, the primary jet expands to the full mixing tube diameter at essentially ambient static pressure.

Since an examination of the plotted test values showed that the difference in performance for the various nozzle locations was very small, it was decided that a primary nozzle position of  $(\theta) = 0$  would give satisfactory results. Further tests were made with the primary nozzle at the above location.

### C. Mixing Section Length and Area Ratio

The purpose of this phase of the test program was to determine the most efficient mixing section length for each of three area ratios. A performance comparison between the mixing tube to primary area ratios,  $(A_3/A_1)$ , was also made. A strain gage diaphragm was added in the secondary plenum chamber to determine the magnitude of the secondary pressure pulsations. The operating conditions and primary nozzle location were determined from section A and B.

Using area ratios of  $(A_3/A_1) = 1.72, 2.48$  and  $4.30$  the mixing section was tested at four lengths of  $(L) = 2-1/2 D_3; 5 D_3; 7-1/2 D_3$  and  $10 D_3$ .

This series of tests was run in a similar manner to those in section B in that five values of thrust and secondary mass flow were obtained for each configuration at five corresponding secondary pressure ratios.

#### 1. Mixing Section Length

The effect of a change in mixing section length upon ejector performance has been plotted in Figures 11, 12 and 13. These data indicate

that the ejector is relatively insensitive to a change in mixing section length ( $L$ ) between the limits  $5 D_3 \leq L \leq 10 D_3$ . The data for a mixing section length of  $2\frac{1}{2} D_3$  shows that the ejector performance has fallen off sharply for the two larger ejector area ratios  $(A_3/A_1) = 4.30$  and  $2.48$ . Thus, for a given value of secondary pressure ratio  $(P_2/P_a)$ , the available mass flow ratio  $(W_2/W_1)$  decreases with mixing section lengths below  $(L) = 5 D_3$ . At  $(A_3/A_1) = 1.72$ , a small decrease in performance is apparent.

To determine the optimum mixing tube length, cross plots of Figures 11, 12 and 13 were made. A typical value of mass flow ratio  $(W_2/W_1)$  of 0.25 and pressure ratio  $(P_2/P_a)$  of 0.75 were chosen and separately held constant. By this method it was possible to obtain curves of secondary pressure ratio and mass flow ratio versus mixing tube length for each of the three area ratios. The results of these cross plots are presented in Figures 14 and 15. Irrespective of the three area ratios tested, maximum performance was obtained for a mixing section length  $(L) = 7.8 D_3$ . On the basis of the configurations tested it can be concluded that any mixing section length  $(L)$  from 6 to  $10 D_3$  will give acceptable performance with a rapid decrease for lengths less than  $5 D_3$ . As mentioned in section B and shown by these curves, a variation in the primary nozzle location will have almost no effect upon the effective mixing section length for values of  $(L)$  greater than  $7 D_3$ .

## 2. Area Ratio

Some of the effects of area ratio on the performance range of an ejector with constant primary flow are also shown in Figures 11, 12 and 13. These data indicate that the slope of the mass flow ratio versus secondary pressure ratio curve increase with area ratio. However, the pressure intercept at  $(W_2/W_1) = 0$ , which represents the minimum secondary vacuum, increases with increasing area ratio.

Determination of the optimum area ratio was carried out by making cross plots of Figures 11, 12 and 13 at typical values of pressure ratio and mass flow ratio. Values were plotted for each of the four mixing

sections lengths tested and are shown in Figures 16 and 17. Maximum performance for the different mixing sections tested was obtained at an area ratio of  $(A_3/A_1) = 2.48$  with the optimum lying between 2.4 and 2.7. Maximum performance would be obtained by using an area ratio of  $(A_3/A_1) = 2.5$ , and a mixing section length of  $(L) = 7.5 D_3$ . For any condition other than optimum, particularly for mixing section lengths less than  $5 D_3$ , performance decreases rapidly.

Performance of the ejector for a number of mass flow ratios, secondary pressure ratios, and area ratios at a constant primary pressure ratio of  $(P_1/P_a) = 1.91$  and primary temperature ratio of  $(T_1/T_a) = 3.32$  has been predicted in Figure 18. A family of curves for constant secondary pressure ratio was developed by cross plotting, which enables one to predict performance at a given area ratio. The curves show that there is an optimum area ratio for maximum mass flow ratio at a given pressure ratio. It can also be seen that, as could be expected, the curve of maximum mass flow ratio moves to the right or the area ratio increases as the pressure ratio is increased. The curves are not completely defined since only four area ratios were tested. Before exact prediction of performance could be obtained several more area ratios would have to be tested,

### 3. Thrust Performance

In addition to ejector performance data for the above configurations, thrust data was also obtained. Readings were obtained from the strain gage balance system, as mentioned in Section II of the report. The results of this data is shown in Figures 19, 20 and 21.

If we consider each of the three area ratios, it is seen that in general, as the area ratio is increased the effect of a change in mixing section length on the thrust decreases at a given secondary pressure ratio. As the area ratio becomes larger, the loss of thrust is increased for a particular configuration, and it was found that keeping the mixing section length at a minimum gave maximum thrust. For any configuration tested, it appears that it would be possible to obtain the equivalent

bare engine thrust if  $(P_2/P_a) \cong 0.95$ , with a possibility of thrust augmentation at  $(P_2/P_a) > 0.95$ . For the point of minimum secondary pressure ratio at zero mass flow the thrust loss increases 35 to 75% as the area ratio is increased from 1.72 to 4.30.

While running the above series of tests, a strain gage diaphragm was mounted on the upper section of the back plate of the plenum chamber, as shown in Figure 2, to record the magnitude of the secondary pressure pulsations. The apparatus was run at a pressure ratio of  $(P_1/P_a) = 1.91$  and 1.62, with a combustion temperature ratio of  $(T_1/T_a) = 3.32$ . The geometric configuration used was typical of those used and was a mixing tube diameter of  $D_3 = 5"$ , length  $(L) = 7.5 D_3$  and  $(\theta) = 0$ . From the test results it was concluded that any secondary pressure pulsations are insignificant. The only great change is at maximum suction where the secondary mass flow is zero. This test condition shows pulsations of varying magnitude. The pulsations of the greatest magnitude have a amplitude equivalent to 0.075" Hg. The frequency of the pulsations is approximately 60 cycles per second.

#### D. Primary Temperature and Pressure

To determine the performance for a given ejector at varying primary operating conditions, particularly the effect of temperature, a series of test runs were made. A geometric configuration of  $(A_3/A_1) = 1.72$  and mixing section length  $(L) = 7.5 D_3$  with primary nozzle in a position of  $(\theta) = 0$ , was used during these tests.

##### 1. Constant Primary Pressure

These runs were made by holding the primary pressure constant at  $(P_1/P_a) = 1.91$  while varying the primary temperature ratio from  $(T_1/T_a) = 1.09$  to  $(T_1/T_a) = 3.92$ . Test results are plotted as Figure 22. This figure shows clearly that at a constant primary pressure ratio, variation of the primary temperature ratio does not effect the mass flow ratio obtainable at different secondary pressure ratios. A closer examination of the above conclusion, drawn from the experimental data, indicates that the ejector

performance must be dependent upon the momentum of the primary mass of air, rather than its kinetic energy. A more detailed discussion and its implications is given in Appendix B.

Thrust versus secondary pressure ratio at constant primary pressure is plotted as Figure 23. A variation of primary temperature at constant primary pressure produces a finite loss in thrust as the temperature is increased. An increasing difference in thrust obtainable at different primary temperatures exists as the secondary pressure ratio is increased, since  $\Delta F = 7$  and  $14$  pounds at  $(P_2/P_a) = 0.40$  and  $0.90$  respectively. In all cases, maximum thrust at a given secondary pressure ratio was obtained at the lowest temperature and decreased as the temperature was raised. It is probable that internal wall friction and turbulence produces the loss in thrust since both increase as the primary temperature becomes higher.

## 2. Constant Primary Temperature

In this series of tests the primary temperature ratio was held constant at  $(T_1/T_a) = 3.32$ , while the primary pressure varied. Mass flow ratio versus secondary pressure ratio at constant primary temperature is plotted as Figure 24. It is seen that the range of secondary pressure ratios available at a given mass flow ratio increases as the primary pressure ratio is increased up to  $(P_1/P_a) = 1.91$ . Apparently a new parameter takes effect as the primary pressure ratio is increased above this value. The cause of this change is probably due to a choking phenomena in the mixing section, and is discussed more fully in the next section.

A plot of the thrust versus secondary pressure ratio with the primary temperature held constant is shown as Figure 25. It appears that the loss in thrust for a given secondary pressure ratio is independent of a change in primary pressure since the curves are parallel. The actual percentage loss decreases with increasing primary pressure ratio. A thrust equal to that of the bare engine would be obtained at values of secondary pressure ratio approximately equal to  $0.95$  for the highest three primary

test pressures. At values of  $(P_2/P_a)$  greater than 0.95 thrust augmentation can be expected.

### 3. Constant Primary Mass Flow

Test runs made at constant primary pressure (Part 1) indicated that the ejector performance is a function of the momentum of the primary jet. Additional tests were made to determine the effect of the heat addition to a primary jet of constant mass flow. A series of runs were made in this manner by varying the primary temperature directly and adjusting the primary pressure to maintain the mass flow.

The similarity between the curves drawn from these runs, Figures 26 and 27, and those drawn for varying primary pressure, Figures 24 and 25, should be noted. Actually the effect of a heat addition to a primary jet of constant mass flow is to increase the total primary pressure. The test results again show that the primary total pressure or momentum is the important ejector parameter. In both sets of test results, it can be noted that at a primary pressure ratio above  $(P_1/P_a) = 1.91$ , a decided change takes place in the flow conditions. If the geometry of the system is considered, it seems likely that a choking is occurring somewhere in the ejector mixing tube. To determine the possibility of this taking place, a number of theoretical calculations were made.

The first possibility considered was that the flow may have reached sonic velocity at the exit of the mixing tube which would cause a choking effect. If we do not consider heat transfer or boundary layer in the tube, and make our calculations with the secondary mass flow,  $W_2 = 0$ , we may derive a formula from the continuity equation giving the relationship between primary mass flow and exit Mach number. This formula and its derivation is given in Appendix C.

For a primary mass flow of  $W_1 = 4.81$  pounds per second obtained at  $(P_1/P_a) = 2.38$ , and  $(T_1/T_a) = 3.72$ , the calculated Mach number was  $M_3 = 0.78$ . A decrease in the temperature due to heat loss would decrease the exit Mach number, but the effect would be small. At the above Mach number, the ratio of the critical or throat area to mixing section area

was  $(A_2/A_3) = 0.955$ , and if sufficient build-up of boundary layer were present, choking would occur at the mixing tube exit. This is probable since only 1/16-inch boundary layer displacement thickness would be required for the 5-inch diameter mixing tube tested.

A second approach to the problem, was to consider the possibility of full expansion of the primary jet to the mixing tube walls. Since the actual geometric area ratio of the primary nozzle and the mixing tube is  $(A_1/A_3) = 0.596$ , full expansion of the jet after leaving the primary nozzle would produce a Mach number of  $(M) = 1.99$ . If the secondary static pressure ratio is determined from the Mach number and the primary pressure, we find that the secondary pressure ratio is  $(P_2/P_a) = 0.322$ , at a primary pressure ratio of  $(P_1/P_a) = 2.38$ . By consulting Figure 28, where the secondary pressure ratio is plotted versus primary ratio at various mass flow ratios, it is seen that a value of secondary pressure ratio of  $(P_2/P_a) = 0.380$  was obtained at a secondary mass flow equal to zero. This indicates that the primary mass was not expanded fully to the mixing section wall unless a pressure lower than  $(P_2/P_a)$  exists in the mixing tube. If we consider the effect of the addition of a finite amount of secondary mass flow, there is a definite possibility that a restriction on the primary jet expansion can exist.

It is of interest to note that choking of the primary nozzle is not a limiting factor in the ejector performance. In the case of the ejector, the primary flow is exhausting into a local low pressure at the entrance of the mixing tube. This local static pressure is essentially equal to the secondary pressure,  $P_2/P_a$ , as shown in the data of Figures 33, 34 and 35. Thus, for a choked primary flow  $P_2/P_a \leq 0.528 P_1/P_a$ . The data of Figure 28 shows that the secondary pressure ratio decreases to a value far lower than  $0.528 P_1/P_a$ , or until limited by a mixing tube phenomena.

#### E. Performance with Diffuser

In an effort to evaluate the benefits that could be derived from the addition of an efficient conical diffuser, a series of tests were made with constant primary conditions, but varying ejector geometry.

Primary conditions were held constant at a primary pressure ratio of  $(P_1/P_a) = 1.91$ , and a primary temperature ratio of  $(T_1/T_a) = 3.32$  to allow a comparison with previous data obtained without the diffuser. The primary nozzle position was set at  $(\theta) = 0$  as used in previous tests. All diffusers had a half angle of  $3-1/2^\circ$ , and area ratios of  $(A_D/A_3) = 6.25; 4.34; 2.44$ , for mixing section area ratios of  $(A_3/A_1) = 1.72; 2.48; \text{ and } 4.30$ ; respectively.

The effect of the addition of a diffuser at the exit of the mixing tube upon mass flow ratio, and secondary pressure ratio for various area ratios, is shown by the data presented in Figures 29, 30 and 31. As can be seen from these curves the addition of a diffuser causes the entire ejector operation curve to shift to the left while still retaining approximately the same slope. Thus, the addition of a diffuser will produce a substantial increase in mass flow ratio at a constant secondary pressure ratio. From the test data an average increment of  $\Delta(W_2/W_1) = 0.80; 0.36; 0.40$ , increase was obtained for area ratios of  $(A_3/A_1) = 1.72; 2.48; \text{ and } 4.30$  respectively at constant secondary pressure ratio. With a constant mass flow ratio, an average decreasing increment of secondary pressure ratio or increasing vacuum was  $\Delta(P_2/P_a) = 0.12; 0.22; \text{ and } 0.05$ , respectively, for the above area ratios. Thus, a diffuser will produce a definite improvement in secondary pressure ratio for a constant mass flow ratio.

In a second series of runs as area ratio of  $(A_3/A_1) = 1.72$  was chosen and held constant while the mixing section length was changed. The purpose of this test was to determine the effect the diffuser produced upon performance at varying mixing section lengths. Actual lengths were  $(L) = 0 D_3, 2.5 D_3, 5 D_3, 7.5 D_3, 10 D_3$ . The results of this test are shown in Figure 32. The addition of a diffuser produces an increase in general performance (both mass flow ratio and secondary pressure ratio) irrespective of the mixing section length. The use of a diffuser allows the section lengths to be considerably shortened since an  $(L) = 2.5 D_3$  gives performance equal to, or better than the longer lengths. The effect of wall friction in the mixing tube is apparent at the higher

mass flows since as the mixing section length is increased, there is a slight drop in mass flow ratio at a given secondary pressure ratio. In a special test run with a mixing section length of  $(L) = 0 D_3$ , or with the diffuser connected directly to the entrance cone, the performance of the ejector was on a par with the longer lengths at high values of secondary pressure ratio or at a low vacuum condition, but drops off considerably in the intermediate range.

As could be expected, the addition of a diffuser reduced the thrust of the system to a small percentage of its value without a diffuser. Thus, the system with a diffuser has no practical application to the tail pipe of a turbo jet or where thrust is an important factor. Possible application lies in a system where mass flow is of primary consideration, and where thrust is not important or obtained in some other manner than the jet itself.

#### F. Pressure Distribution Along Mixing Tube

In an attempt to study the internal flow process within the ejector mixing tube a series of static pressure measurements were obtained along the mixing section length. It was realized that a pitot-static survey would be necessary for a complete study of the mixing process, however, the static wall surveys gave several significant indications.

Pressure distribution along the mixing tube for area ratios of  $(A_3/A_1) = 1.72$ , and a length of  $(L) = 5.0 D_3$  is shown in Figures 33, 34 and 35 for mass flow ratios of  $(W_2/W_1) = 0.00, 0.15$  and  $0.30$ . For the diffuser configuration at zero secondary mass flow or  $(W_2/W_1) = 0$ , the flow apparently expands rapidly to the mixing tube wall as indicated by pressure discontinuity at approximately one diameter downstream. This is probably an oblique compression shock generated at the wall necessary to turn the expanded flow to a direction parallel to the mixing tube wall. Beyond a mixing section length of two diameters a fairly constant supersonic flow appears to be established in the mixing tube. Since the flow is non-isentropic, the actual Mach number can not be determined from the static readings alone. With secondary flow  $(W_2/W_1) = 0.15$  and  $0.30$ , no

pressure discontinuities at the wall are apparent. The primary flow apparently expands less rapidly, and is accompanied by acceleration of the secondary flow in the mixing tube. The gradual increase in static wall pressure is probably due to the continuation of the mixing process. In the case of the  $(W_2/W_1) = 0.00$  and  $0.15$  the mixing tube flow appears to remain supersonic with a normal shock probably at the diffuser entrance. At  $(W_2/W_1) = 0.30$ , the mixed flow may be either in the high subsonic or low supersonic regime.

In the case of no diffuser the primary flow apparently decelerates through a series of progressively weakening oblique shock waves without expansion to the mixing section walls in all cases. The mixed flow is subsonic with the condition  $(P_x/P_a) = 1$ , at the exit of the mixing tube. A similar process is apparent in the data presented in Figures 36 through 39, both with and without diffuser. These data were run with mixing tube area ratios of  $(A_3/A_1) = 2.48$  and  $4.30$  at  $(L) = 7.5 D_3$ . In these cases the addition of a diffuser permits the mixing section pressure to be reduced, since the diffuser allows  $(P_x/P_a) = 1$  at the diffuser exit.

Internal mixing section wall pressure distribution data for length of  $(L) = 2.5 D_3$ ,  $5.0 D_3$ ,  $7.5 D_3$  and  $10 D_3$  at  $(A_3/A_1) = 1.72$  are presented in Figures 40 through 42.

Pressure distribution data without diffuser for the various mixing section lengths are practically superimposed. If the establishment of the exit condition of  $(P_x/P_a) = 1$  is assumed to be an indication of the completion of the mixing process, the data presented indicates that  $(L) = 5.0 D_3$  is sufficient at  $(W_2/W_1) = 0.15$  and  $0.30$ , since beyond this length  $(P_x/P_a) = 1$ . Ejector performance data, Figures 11 through 21 established an optimum mixing tube length of  $(L) = 7.5 D_3$ . However, small differences were noted at  $(L) = 5.0 D_3$  but decreased considerably at  $(L) = 2.5 D_3$ . Thus, the performance and wall pressure tests appear to be in reasonable agreement.

Pressure distribution data with diffuser show relatively small changes with mixing tube length. At all three mass flow ratios  $(W_2/W_1) = 0.00$ ,  $0.15$ , and  $0.30$ , a higher wall pressure exists beyond  $(D_x/D_3) = 3.0$  for the  $(L) = 10 D_3$  configuration as compared to  $(L) = 5 D_3$ . This may be due to an increased boundary layer built up in the case of the longer mixing length which could materially lower the diffuser efficiency and static pressure recovery. The difference is particularly large at  $(W_1/W_2) = 0.30$ , where all measured static pressures are appreciably higher at  $(L) = 10 D_3$ .

#### IV. CONCLUSIONS

The purpose of this research program was to analyze and determine the geometric and state parameters of a hot gas ejector system. The conclusions that may be drawn from this research are summarized as follows:

1. The performance of the ejector is relatively insensitive to primary nozzle position ( $Q$ ) between the limits of one mixing tube diameter ( $D_3$ ) downstream and one-half diameter upstream of the entrance to the mixing section length. Ejector performance definitely decreased for a primary nozzle position equal to one diameter upstream for secondary to primary area ratios of  $(A_3/A_1) = 1.72$  and  $2.48$ , but showed no significant change at  $(A_3/A_1) = 4.30$ . The range of secondary to ambient pressure ratio  $(P_2/P_a)$  extended from  $0.45$  to  $0.94$  and secondary to primary mass ratio  $(W_2/W_1)$  from  $0$  to  $0.45$  during tests to determine optimum primary nozzle location.
2. Optimum mixing section length irrespective of area ratio is seven to eight times the diameter of the mixing tube.

Excluding mixing section lengths shorter than  $(L) = 5 D_3$ , the performance of the ejector is relatively insensitive to a change in mixing tube length.

3. It was found that the optimum area ratio ( $A_3/A_1$ ) lies between 2.4 and 2.7 for fixed primary conditions of  $(P_1/P_a) = 1.91$ , and  $(T_1/T_a) = 3.32$ . No secondary flow was obtained for the smallest area ratio tested,  $(A_3/A_1) = 1.09$ . Evidently, the low mixing section to primary nozzle area ratio is not sufficient to allow the induction of any appreciable mass flow.
4. The relative effect on mass flow ratio and thrust for a change in mixing section length decreases as the area ratio is increased. The loss of thrust, when operating the system, becomes larger as the area ratio is increased. Mixing section length should be kept at a minimum for maximum thrust. At very high secondary pressure ratios  $(P_2/P_a) \geq 0.95$ , it may be possible to obtain a small amount of thrust augmentation from the system.
5. For the configurations tested, maximum performance was obtained for an area ratio  $(A_3/A_1) = 2.48$  and a mixing section length of  $(L) = 7.5 D_3$ , with a primary nozzle location of  $(\ell) = 0$ .
6. Secondary pressure pulsations are insignificant, and the pulsations of the greatest magnitude occur at a test condition where the secondary mass flow is zero or at maximum suction.
7. For a fixed ejector geometry and at constant primary pressure ratio, variation of the primary temperature does not affect the secondary mass flow obtainable at different secondary pressure ratios. This indicates that ejector performance depends entirely upon the momentum of the primary mass flow. Maximum thrust was obtained at the lowest temperature. Wall friction and mixing losses apparently reduce the thrust as the temperature increases.

8. Performance of the ejector is determined by the primary pressure ratio. The decrease in thrust as the secondary pressure ratio is decreased for constant primary temperature, is determined by the geometric configuration, and is independent of a change in primary pressure. The range of secondary pressure ratios will increase as the primary pressure is increased to an optimum value. This optimum value of primary pressure ratio for a given geometry is determined by the mass flow ratio desired and above this optimum a choking effect takes place which causes the performance to decrease rapidly. Optimum ejector performance for a given range of primary operating conditions is primarily a function of ejector geometry and secondary mass flow. Knowledge of heat transfer ratios and boundary layer built up in the mixing tube are necessary for exact ejector performance predictions.
9. The addition of a diffuser upon the exit of the mixing tube produced a substantial increase in ejector performance. Both mass flow ratio and secondary pressure ratio were improved irrespective of the mixing section length. In fact, the diffuser almost completely neutralizes the effect of the mixing section. This increase in performance is obtained at a sacrifice of all but a small percentage of the thrust. Thus, a system equipped with a diffuser has no practical application in a system where thrust loss is of importance.
10. Pressure distribution tests made along the mixing tube indicate that the use of a diffuser maintains supersonic flow the entire length of the mixing section at  $(A_3/A_1) = 1.72$ , and the flow is reduced to subsonic by a normal shock in the diffuser. The distribution also shows the effectiveness of the mixing process between the two flows. Mixing apparently is nearly complete within five diameters downstream irrespective of the actual mixing section length.

11. The ejector test program has served to eliminate several geometric variables such as primary nozzle location and mixing section length, but it does not provide a complete set of data to cover all jet operational conditions.

The example considered in Appendix D shows that further testing at several more area ratios over a range of primary pressures of 1.0 to 4.0 would be required for a complete application analysis. Consideration of special nozzle designs to reduce the thrust loss to a minimum would also be desirable.

REFERENCES

1. An Experimental Investigation of Rectangular Exhaust Gas Ejectors Applicable for Engine Cooling, Manganiello, Eugene J. and Bogatsky, Donald. NACA ARR E4E31, May, 1944 (E-224).
2. Effect of Temperature on Performance of Several Ejector Configurations, Welsted, N. D., Huddleston, S. C., and Ellis, C. W., NACA RM #9 #16, June 13, 1949, (Restricted).
3. Analysis of Thrust Augmentation Nozzle for High Velocity Drag Reduction, Weinig, Fredrick, Technical Report G5-OSAF, Wright Patterson Air Base, No. 99 NO. F-TR-2212-ND (Confidential).
4. Experimental Study of Ejectors for Use in Exhausting Ram Jet Test Burners, Currey, Richard, UAC Report No. 32, (Meteor), January, 1949, (Confidential).
5. A Theoretical and Experimental Investigation of Jet Augmentation, Wilder, J. C., Curtiss-Wright Corporation, Report No. BC-357-A-1.
6. Preliminary Investigation of Cooling-Air Ejector Performance at Pressure Ratios from 1 to 10, C. W. Ellis, D. P. Holister, and A. F. Sargent, Jr. NACA RM E 51H21, October 17, 1951, (Confidential).
7. Performance of Several Air Ejectors with Conical Mixing Sections and Small Secondary Flow Rates, S. C. Huddleston, H. D. Wilsted, and D. W. Ellis, NACA RM E8D23, July 19, 1948.
8. Tests on Thrust Augmentors for Jet Propulsion, E. N. Jacobs and J. M. Shoemaker, NACA TN 431, September 1932.
9. Jet Propulsion with Special Reference to Thrust Augmentors, G. B. Schubaner, NACA TN 442, January 1933.
10. Calculation of Airflow Through an Ejector - Operated Engine Cooling System for a Turbojet Powered Aircraft, J. L. Fletcher, Douglas Aircraft Report No. SM-14 020, May 10, 1951.

A P P E N D I X ANOMENCLATURE

- $A_1$  ----- Exit cross-sectional area of primary nozzle.  
 $A_3$  ----- Cross-sectional area of mixing tube section.  
 $A_D$  ----- Exit cross-sectional area of diffuser.  
 $A^*$  ----- Fictitious cross-sectional area of upstream throat.  
 $A_3/A_1$  ----- Area ratio of mixing tube to primary nozzle.  
 $A_D/A_3$  ----- Area ratio of diffuser to mixing section.  
 $D_1$  ----- Diameter of primary nozzle.  
 $D_3$  ----- Diameter of mixing tube.  
 $D_x/D_3$  ----- Distance downstream of entrance of mixing section length in terms of mixing section diameters.  
 $F_e$  ----- Total thrust of the ejector system in pounds.  
 $F_j$  ----- Thrust of the jet (Bare engine) in pounds.  
 $KE$  ----- Kinetic Energy.  
 $\ell$  ----- Primary nozzle location in terms of mixing section diameters up or downstream of entrance to mixing section.  
 $L$  ----- Mixing section length in terms of mixing section diameters.  
 $m_1$  ----- Primary or jet mass flow in slugs per second.  
 $m_2$  ----- Secondary mass flow in slugs per second.  
 $m_3$  ----- Combined primary-secondary or ejector mass flow in slugs per second.  
 $M_3$  ----- Mach number at the exit of the mixing tube.  
 $P_a$  ----- Local atmosphere pressure.  
 $P'_a$  ----- Minimum pressure ratio for NACA 66, - (.12) .12 airfoil section  $C_1 = 0.20$ .  
 $P_1$  ----- Total primary pressure.  
 $P_2$  ----- Total secondary pressure.  
 $P_3$  ----- Total pressure at exit of mixing tube.  
 $P_1/P_a$  ----- Ratio of total primary pressure to atmospheric pressure.  
 $P_2/P_a$  ----- Ratio of secondary total pressure to atmospheric or free stream pressure.

$p_1$ -----	Static primary pressure.
$p_2$ -----	Static secondary pressure.
$p_3$ -----	Static pressure at exit of mixing tube.
$p_x$ -----	Static pressure along the mixing section length.
$p_x/p_a$ -----	Ratio of pressure along mixing tube to atmospheric pressure.
$R$ -----	Gas constant $1715 \text{ ft}^2 \text{ sec}^2 / \text{°R}$ .
$T_a$ -----	Ambient air temperature.
$T_1$ -----	Total temperature of primary mass flow.
$T_2$ -----	Total temperature of secondary mass flow.
$t_3$ -----	Static temperature at mixing tube exit.
$T_3$ -----	Stagnation temperature at mixing tube exit.
$T_1/T_a$ -----	Ratio of primary to ambient temperatures.
$T_1/T_2$ -----	Ratio of primary to secondary temperatures.
$V_1$ -----	Velocity of the primary jet mass flow.
$V_2$ -----	Velocity of secondary mass flow, approximately equal to zero in plenum chamber.
$V_3$ -----	Velocity of combined primary and secondary flow at the exit of the mixing tube.
$W_1$ -----	Weight flow of primary stream in pounds per second.
$W_2$ -----	Weight flow of secondary stream in pounds per second.
$W_2/W_1$ -----	Weight or mass flow ratio of secondary to primary flows.
$\rho$ -----	Density of air in the free stream, slugs per cubic foot.
$\gamma$ -----	Ratio of Specific heats, $c_p/c_v$ , (1.4 for air).
$a_3$ -----	Velocity of sound at $t_3$ .
$a_{03}$ -----	Velocity of sound at $T_3$ .

A P P E N D I X B

DERIVATION OF MOMENTUM RELATION

One of the conclusions derived from the tests made at constant primary pressure was that a variation of the primary temperature did not affect the mass flow ratio obtainable at any given secondary pressure ratio. It may be inferred from this result that the ejector performance must be dependent upon the momentum of the primary mass of air.

For the primary or inductive flow

$$\text{Mom}_1 = p_1 A_1 + m_1 V_1 \quad (\text{at the nozzle exit})$$

where

$$p_1/p_1 = (1 + \frac{\gamma-1}{2} M_1^2)^{\frac{\gamma}{\gamma-1}}$$

$$m_1 = \rho_1 V_1 A_1 = \rho_{o1} (1 + \frac{\gamma-1}{2} M_1^2)^{\frac{1}{1-\gamma}} V_1 A_1$$

$$V_1 = M_1 a_1 = M_1 a_o (1 + \frac{\gamma-1}{2} M_1^2)^{-1/2}$$

$$\rho_{o1} = \frac{p_1}{RT_1}$$

$$a_o = (\gamma RT_1)^{1/2}$$

thus

$$\begin{aligned} \text{Mom}_1 &= A_1 \left[ p_1 (1 + \frac{\gamma-1}{2} M_1^2)^{\frac{\gamma}{1-\gamma}} + \rho_{o1} M_1^2 a_o^2 (1 + \frac{\gamma-1}{2} M_1^2)^{\frac{\gamma}{1-\gamma}} \right] \\ &= A_1 (1 + \frac{\gamma-1}{2} M_1^2)^{\frac{\gamma}{1-\gamma}} \left[ p_1 + \frac{p_1}{RT_1} \gamma RT_1 M_1^2 \right] \\ &= p_1 A_1 (1 + \frac{\gamma-1}{2} M_1^2)^{\frac{\gamma}{1-\gamma}} \left[ 1 + \gamma M_1^2 \right] \end{aligned}$$

Therefore, for a fixed ejector geometry operating at constant primary pressure ratio and Mach number at the nozzle exit, the momentum is essentially constant over the temperature range investigated,  $520^\circ\text{R} \leq T_1 \leq 1660^\circ\text{R}$ . The variation in " $\gamma$ " over this range has negligible effect. Since constant mass flow ratios, at a given  $P_2/P_a$ , were also obtained, the test results indicate that the ejector performance is a function of the primary or inductive momentum.

A P P E N D I X C

DERIVATION OF EXIT MACH NUMBER EQUATION

During tests made with a constant primary temperature it was noted that as the primary pressure ratio  $P_1/P_a$  was increased to values greater than 1.91, a new effect is apparent in ejector performance for the configuration tested. Consideration of the possibilities that would cause this effect indicated that a choking condition could be taking place within the mixing tube.

To determine this possibility it was first considered that the flow may have reached sonic velocity at the exit of the mixing tube. By not considering heat transfer or boundary layer buildup in the tube, and making our calculations for a secondary mass flow of  $W_2 = 0$ , we can derive a formula relating the primary mass flow and Mach number.

From the continuity equation we have:

$$W_1 = \rho_3 V_3 A_3.$$

where

$W_1$  = Primary weight flow

$\rho_3$  = Exit density

$V_3$  = Exit velocity

$A_3$  = Exit area

and

$$V_3 = M_3 a_3$$

$$a_3 = 49.1 (\sqrt{t_3})$$

$$\rho_3 = \frac{P_3}{Rt_3} = \frac{P_a}{Rt_3}$$

Then

$$W_1 = \frac{P_a}{Rt_3} a_3 M_3 A_3$$

where

$$t_3 = T_3 \left(1 + \frac{\gamma-1}{2} M_3^2\right)^{-1}$$

$$a_3 = a_{03} \left(1 + \frac{\gamma-1}{2} M_3^2\right)^{-1/2}$$

$$a_{03} = 49.1 (T_3)^{1/2}$$

We obtain

$$W_1 = \frac{P_a}{RT_3} 49.1 (T_3)^{1/2} \left(1 + \frac{\gamma-1}{2} M_3^2\right)^{1/2} M_3 A_3$$

since  $T_3 = T_1$  neglecting heat transfer

$$W_1 = \frac{49.1}{R} P_a A_3 \cdot M_3 \left(\frac{1 + \frac{\gamma-1}{2} M_3^2}{T_1}\right)^{1/2}$$

Thus, the exit Mach numbers may be calculated from primary operating conditions and ejector geometry.

A P P E N D I X D

EJECTOR THRUST AS PREDICTED BY THE MOMENTUM EQUATION

The general momentum equation for an ejector configuration as shown in Figure 2 can be written as follows:

$$(1) \quad m_1 V_1 + p_1 A_1 + m_2 V_2 + p_2 A_2 = m_3 V_3 + p_3 A_3$$

The nomenclature for the above terms is given in Appendix A.

In equation (1) the jet thrust,  $F_j = m_1 V_1$

the ejector thrust  $F_e = m_3 V_3$ .

Also

$$A_3 = A_1 + A_2 \qquad m_3 = m_1 + m_2 \qquad p_3 = p_a$$

equation (1) can be written

$$(2) \quad F_e - F_j = m_1 (V_3 - V_1) + m_2 V_3 = p_a \left[ A_1 (p_1/p_a - 1) - A_2 (1 - p_2/p_a) \right] + m_2 V_2$$

where  $(F_e - F_j)$  represents a static thrust loss at negative values or a thrust gain at positive values. The important parameters to avoid a thrust loss are evident from equation (2). Thus, for a given ejector operation condition the secondary area,  $(A_2)$ , should be kept to a minimum and the secondary pressure ratio  $(p_2/p_a)$  should be kept at a maximum.

Calculated values of  $(F_e - F_j)$  were determined for a typical set of ejector performance values at  $(L) = 7.5 D_3$  taken from the data of Figure 11. Actual geometric and static conditions from the data were substituted into equation (2), and the theoretical ejector thrust determined. Actual ejector thrust is given in Figure 19. A friction drag for a mixing section length of  $(L) = 7.5 D_3$  was determined by the difference in thrust between  $(L) = 10 D_3$  and  $2.5 D_3$ . This drag was then added to the ejector thrust to give the equivalent frictionless value. The calculated and experimental thrust values are in good agreement as shown in the table below. The comparison serves as a check on the thrust measurements and indicates that the ejector thrust can be calculated within 2 per cent from ejector performance data.

## COMPARISON OF CALCULATED AND MEASURED THRUST

$p_2/p_a$	$W_2/W_1$	$F_e/F_j$ (calculated values) (from Eq. 2)	$F_e/F_j$ (experimental values) (from Fig. 19)
0.5	.055	.776	.765
0.6	.118	.823	.825
0.7	.175	.882	.891
0.8	.234	.942	.952
0.9	.300	1.007	1.016
1.0	.367	1.071	1.076

A P P E N D I X E

APPLICATION OF EJECTOR DATA TO AN AIRCRAFT INSTALLATION

The basic purpose of this experimental program has been to determine the feasibility of utilizing an ejector with a hot exhaust gas primary flow to effect boundary layer removal from aerodynamic surfaces. Of course an important application would be the case of a jet aircraft. The effect of such an application on the thrust of the engine as well as the aerodynamic benefit obtained by boundary layer removal must be considered.

In Figure 43 and 44, ejector data has been applied to a hypothetical jet aircraft installation. The secondary pressure ratio ( $P_2/P_a$ ) as a function of the exhaust pressure ratio ( $P_1/P_a$ ) at constant mass flow ratios from 0.0 to 0.3 has been plotted in Figure 43. Also included is a plot of minimum local pressure on a typical airfoil section as a function of flight Mach number. To effect boundary layer removal from the wing, ejector suction pressure must be lower than ( $P'_a/P_a$ ) at a given flight Mach number. This would probably be a conservative condition since the suction slot location could be to the rear of the minimum pressure point. To effect an ejector mass flow ratio of 0.2 at  $M = 0.80$ , the jet must operate between the limits of  $1.68 < P_1/P_a < 2.40$ . At  $(W_2/W_1) = 0.1$  the range is from  $1.43 < P_1/P_a < 3.00$ . The action of the ejector in conjunction with slot suction would be self adjusting. Assuming zero pressure losses in the duct a jet operating at  $(P_1/P_a) = 2.20$  at low speed, such as at take off when  $(P'_a/P_a) = 1.0$ , the ejector would pump  $(W_2/W_1) = 0.37$ , but at  $M = 0.90$  this would be reduced to 0.21 because of the reduced airfoil pressure  $(P'_a/P_a) = .775$ . Referring to Figure 44, the air craft at take off would then operate at an ejector jet thrust ratio of about 1.03 or at a 3 per cent thrust augmentation. At  $M = 0.90$  with  $(P_1/P_a) = 2.20$  and  $(W_2/W_1) = 0.21$ ,  $(F_e/F_j) = 0.915$ , but the actual thrust loss would exceed the static value since the ejector mixing action has reduced the jet velocity. The importance of this effect increases with increasing flight Mach number.

The example considered in Figures 43 and 44 is for a single ejector area ratio over a limited range of exhaust pressure ratios. It appears that further testing at several area ratios over a range of primary pressures of 1.0 to 4.0 would be desirable for a complete application analysis. During these tests the temperature could be kept constant since this effect has been determined by the present program.

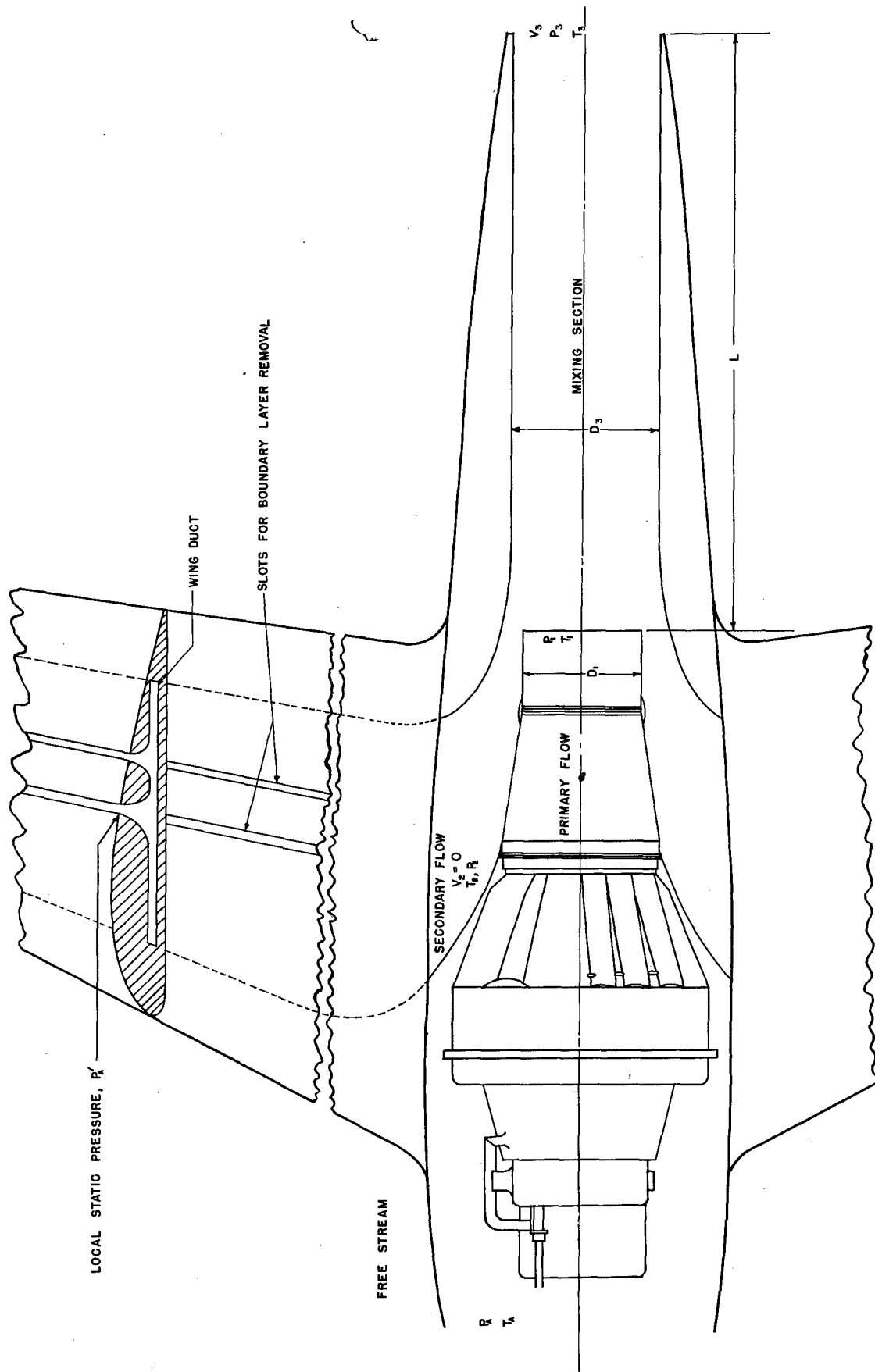
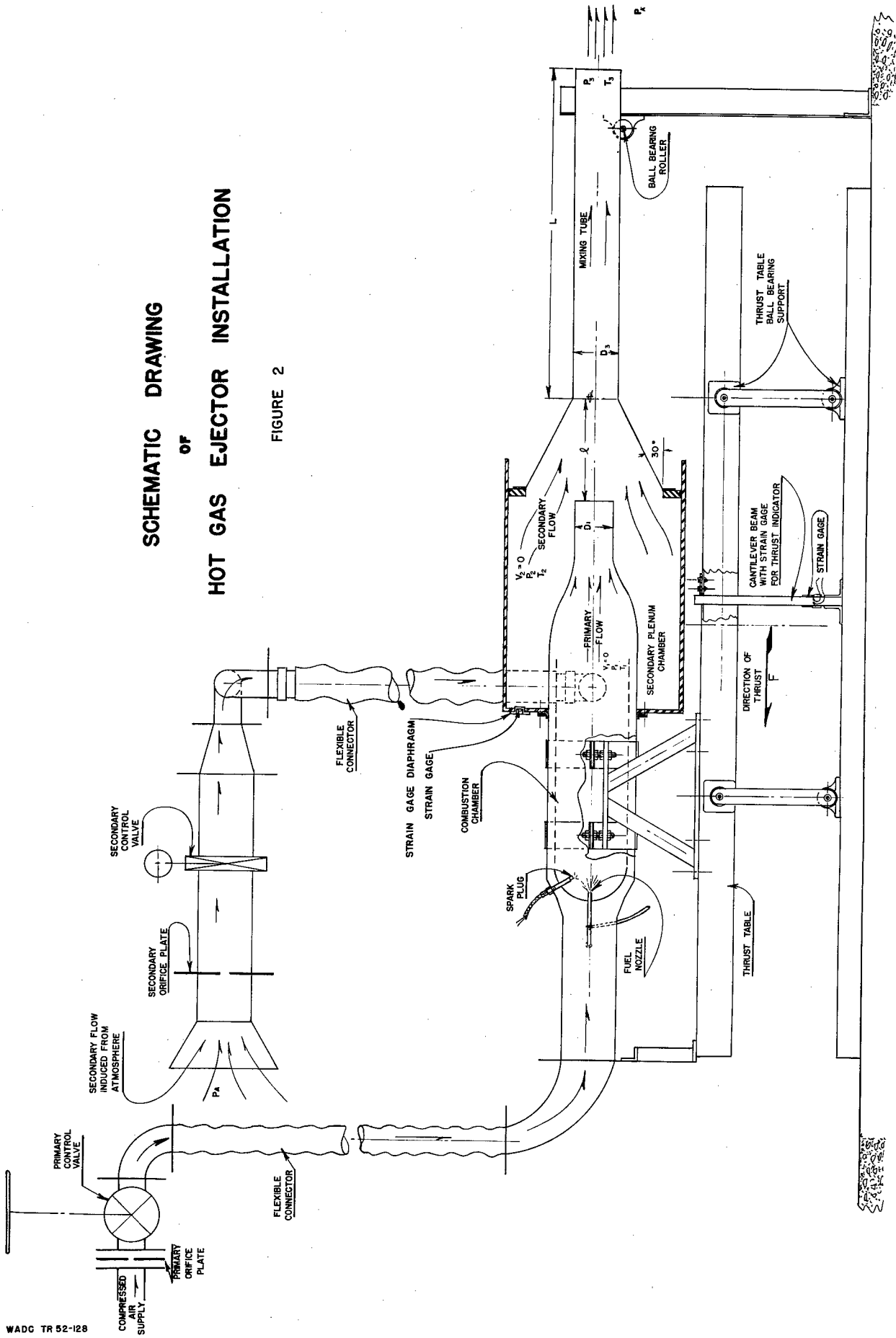


FIGURE 1

SCHEMATIC DIAGRAM OF  
EJECTOR APPLICATION TO TURBO-JET AIRCRAFT  
FOR BOUNDARY LAYER AIR REMOVAL

# SCHEMATIC DRAWING OF HOT GAS EJECTOR INSTALLATION

FIGURE 2



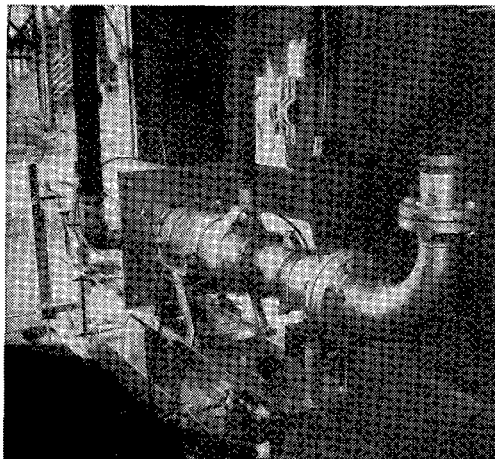


FIGURE 3- FRONT VIEW OF APPARATUS  
SHOWING COMBUSTION CHAMBER AND  
FLEXIBLE HOSE CONNECTIONS.

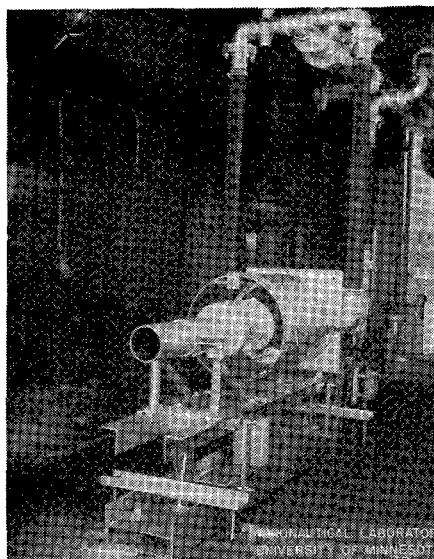


FIGURE 4- REAR VIEW OF TEST  
FACILITY SHOWING CONE AND MIXING  
TUBE OF EJECTOR SYSTEM MOUNTED  
IN THE PLENUM CHAMBER.

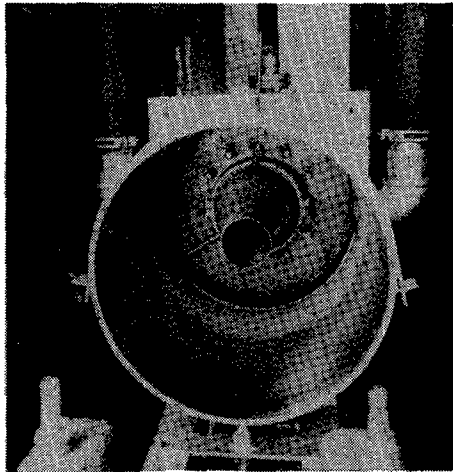


FIGURE 5- CLOSE UP OF BARE PLENUM CHAMBER AND PRIMARY NOZZLE. PRESSURE AND TEMPERATURE PROBES ARE SHOWN MOUNTED IN THE NOZZLE.

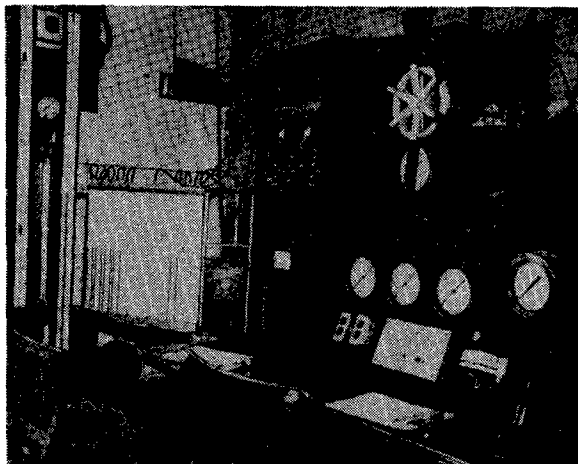
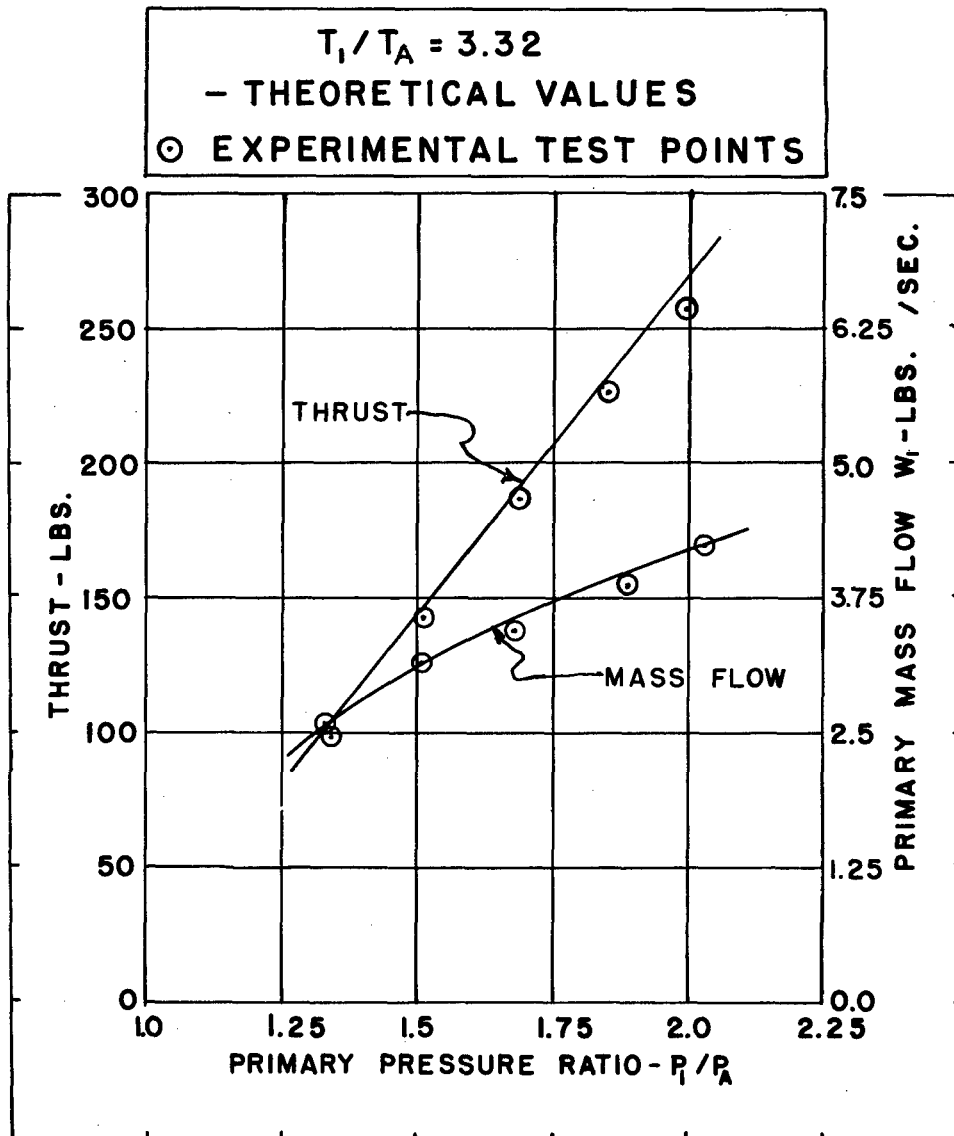


FIGURE 6- RECORDING AND OPERATING INSTRUMENTS IN THE CONTROL ROOM.

FIGURE 7  
 THRUST AND MASS FLOW vs. PRIMARY PRESSURE RATIO



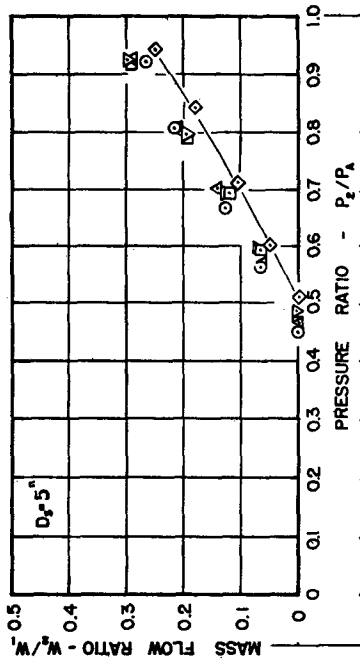
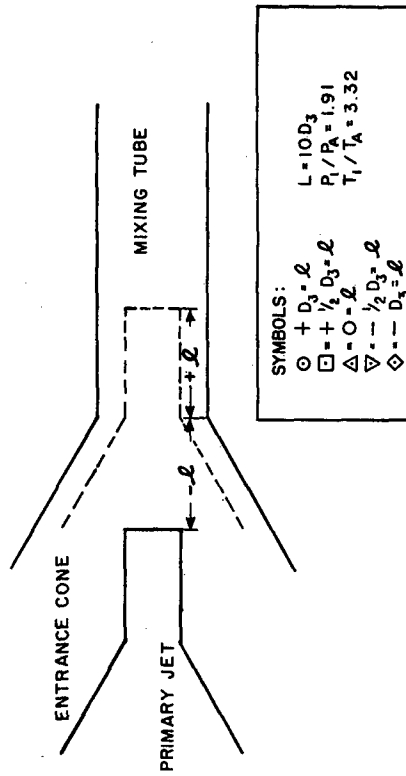


FIGURE 9  
MASS FLOW RATIO vs. SECONDARY PRESSURE RATIO  
 $A_3/A_1 = 1.72$



THE EFFECT OF PRIMARY NOZZLE  
LOCATION ON EJECOR PERFORMANCE

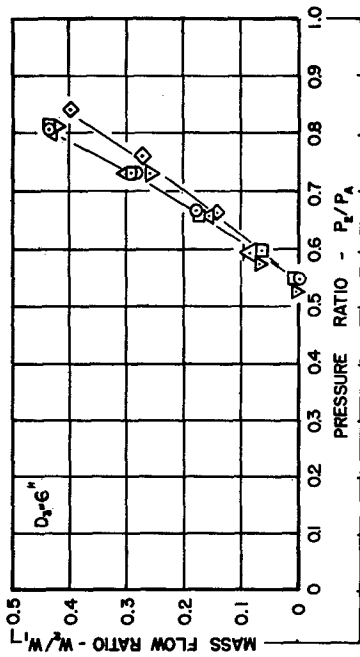


FIGURE 8  
MASS FLOW RATIO vs. SECONDARY PRESSURE RATIO  
 $A_3/A_1 = 2.48$

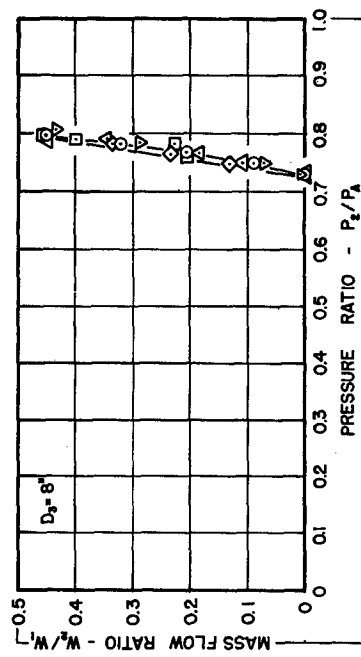


FIGURE 10  
MASS FLOW RATIO vs. SECONDARY PRESSURE RATIO  
 $A_3/A_1 = 4.30$

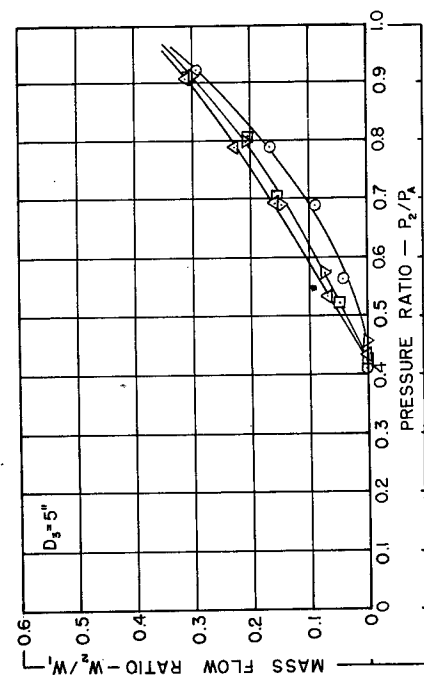


FIGURE 11  
MASS FLOW RATIO vs. SECONDARY PRESSURE RATIO  
 $A_3/A_1 = 1.72$

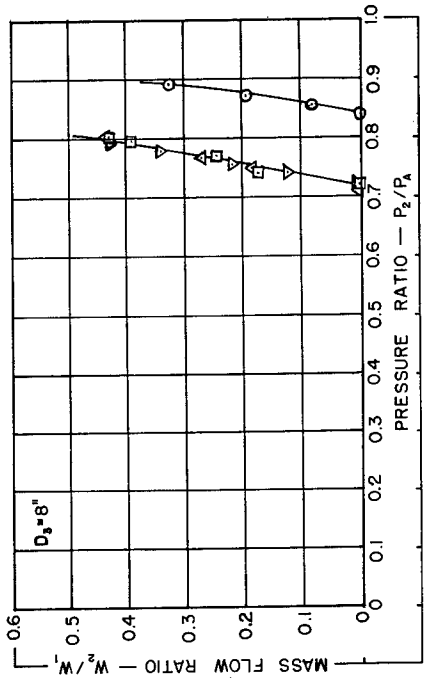


FIGURE 13  
MASS FLOW RATIO vs. SECONDARY PRESSURE RATIO  
 $A_3/A_1 = 4.30$

SYMBOLS:  
 $\circ = 2.5 D_3 = L$   
 $\square = 5.0 D_3 = L$   
 $\triangle = 7.5 D_3 = L$   
 $\nabla = 10.0 D_3 = L$   
 $T_1/T_2 = 3.32$   
 $P_1/P_2 = 1.91$   
 $L = 0$

THE EFFECT OF MIXING TUBE LENGTH ON EJECTOR MASS RATIO

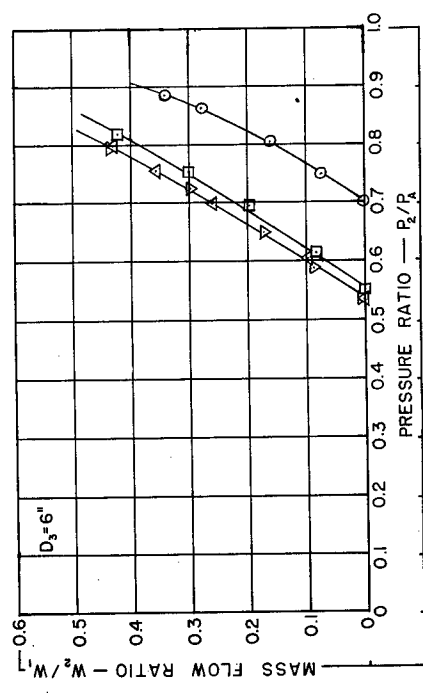


FIGURE 12  
MASS FLOW RATIO vs. SECONDARY PRESSURE RATIO  
 $A_3/A_1 = 2.48$

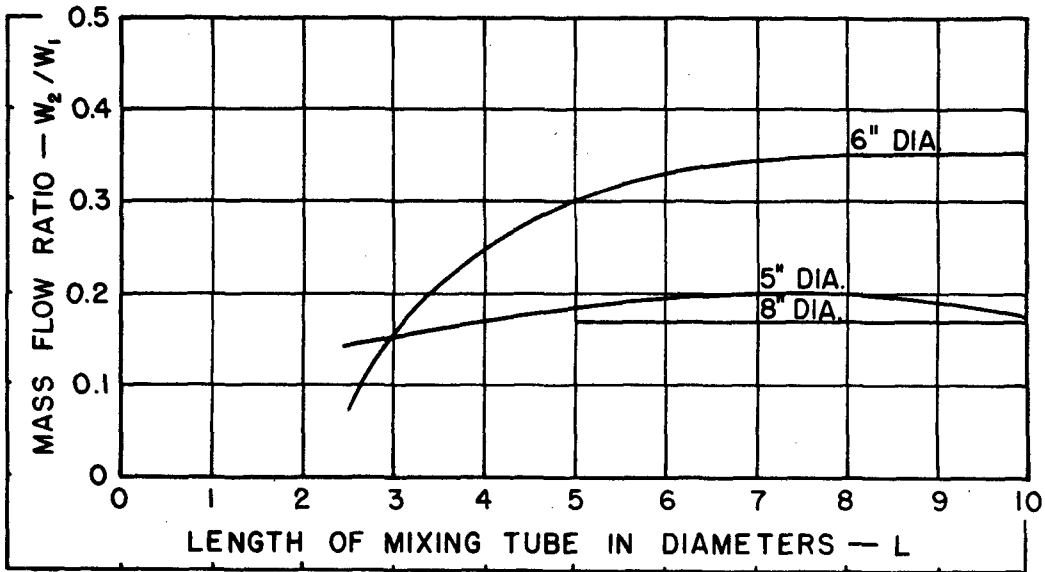


FIGURE 14

MASS FLOW RATIO vs. MIXING TUBE LENGTH AT  $P_2/P_A = .75$

## DETERMINATION OF OPTIMUM MIXING TUBE LENGTH

$l = 0 \quad T_1/T_A = 3.32 \quad P_1/P_A = 1.91$

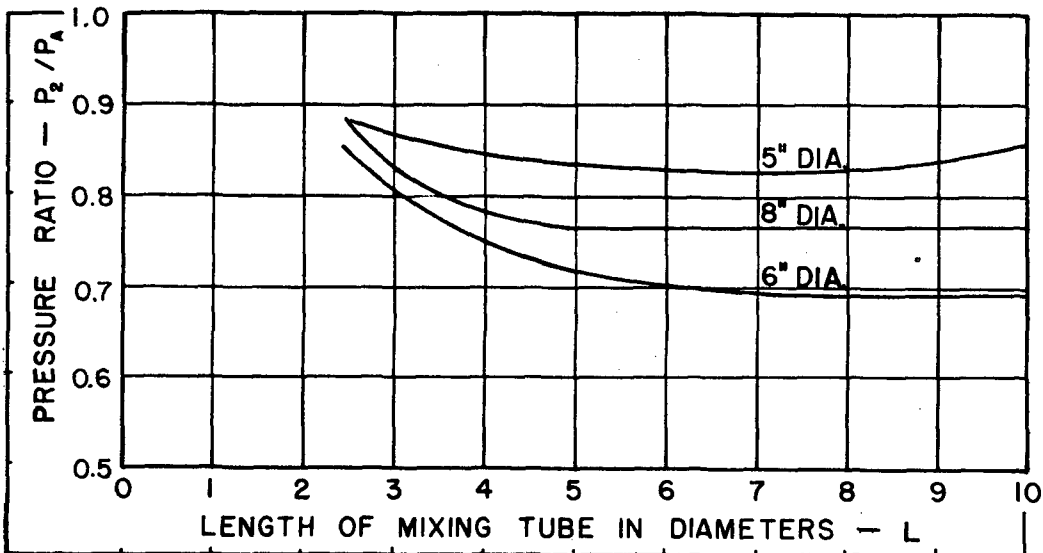


FIGURE 15

PRESSURE RATIO vs. MIXING TUBE LENGTH AT  $W_2/W_1 = .25$

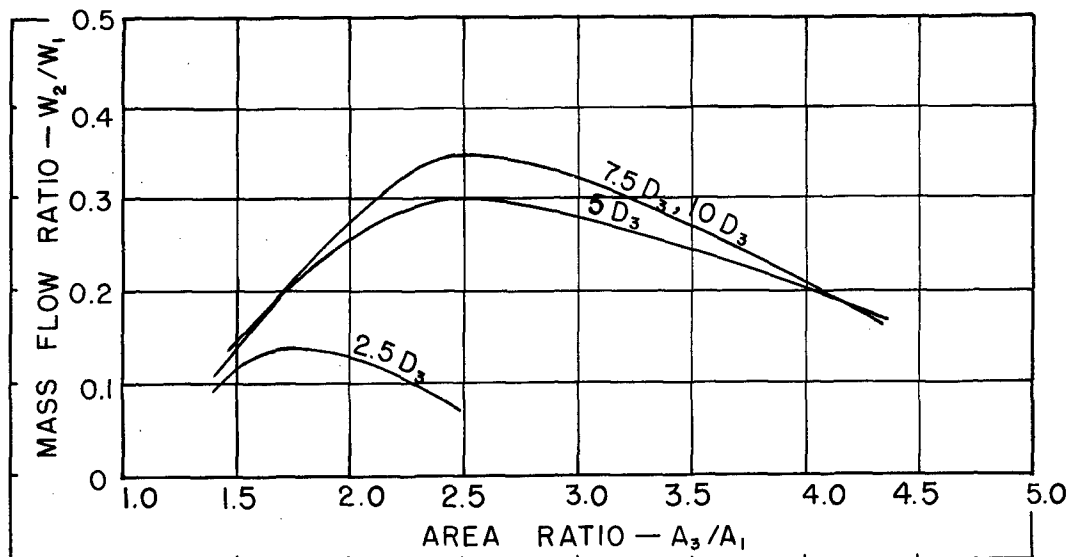


FIGURE 16

MASS FLOW RATIO vs. AREA RATIO AT  $P_2/P_A = .75$

### DETERMINATION OF OPTIMUM AREA RATIO

$l = 0$	$T_1/T_A = 3.32$	$P_1/P_A = 1.91$
---------	------------------	------------------

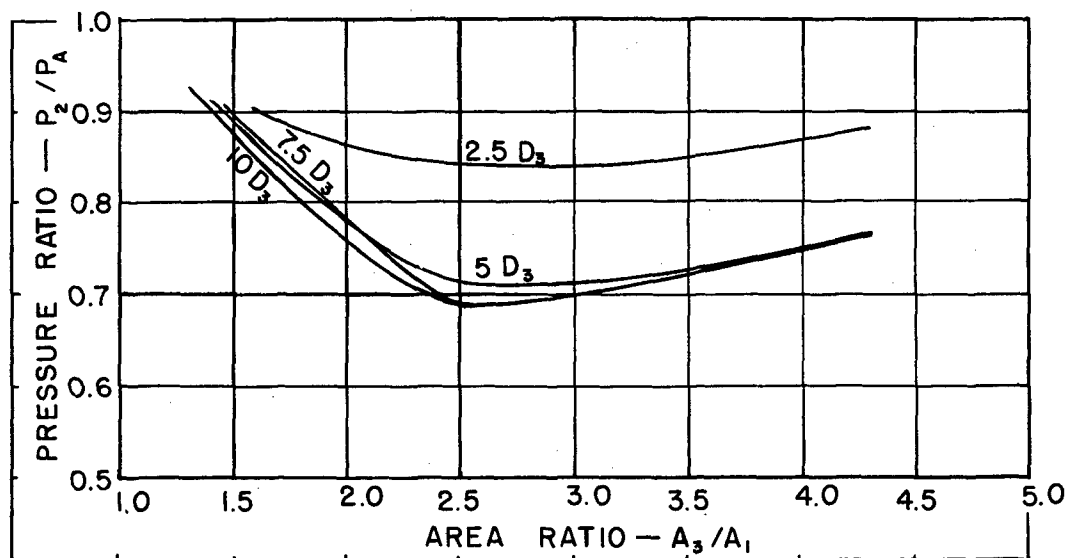


FIGURE 17

PRESSURE RATIO vs. AREA RATIO AT  $W_2/W_1 = .25$

### PREDICTED EJECTOR PERFORMANCE

$A_3/A_1$	1.09	$L = 7.5 D_3$
	1.72	$\theta = 0$
	2.48	$P_1/P_A = 1.91$
	4.30	$T_1/T_A = 3.32$
	$P_2/P_0 = 0.45 \text{ TO } 0.90$	

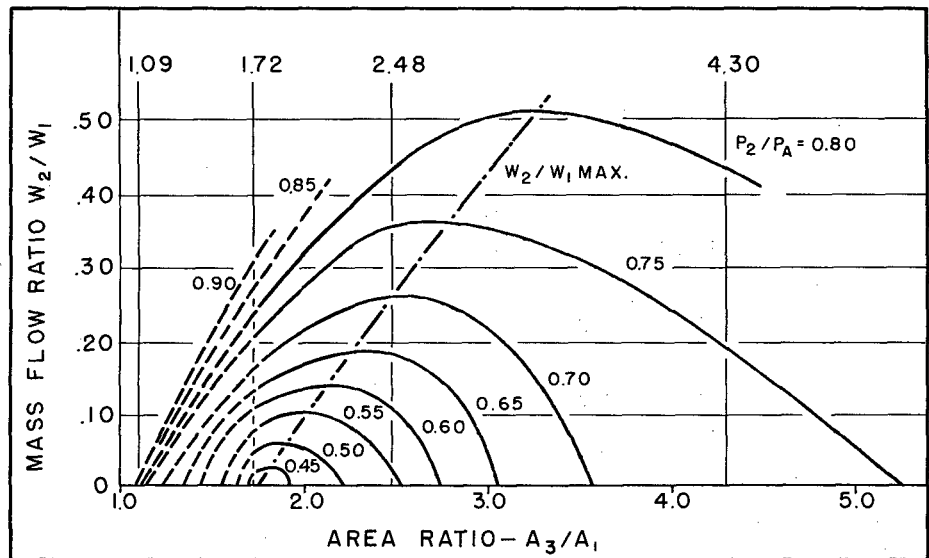


FIGURE 18

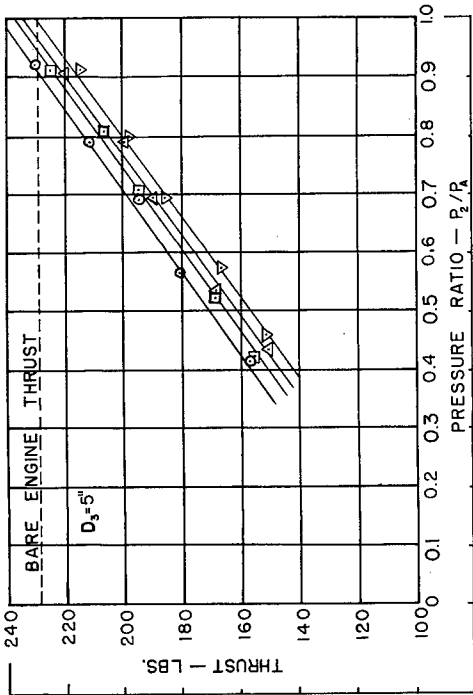


FIGURE 19  
THRUST vs. SECONDARY PRESSURE RATIO  
 $A_3/A_1 = 1.72$

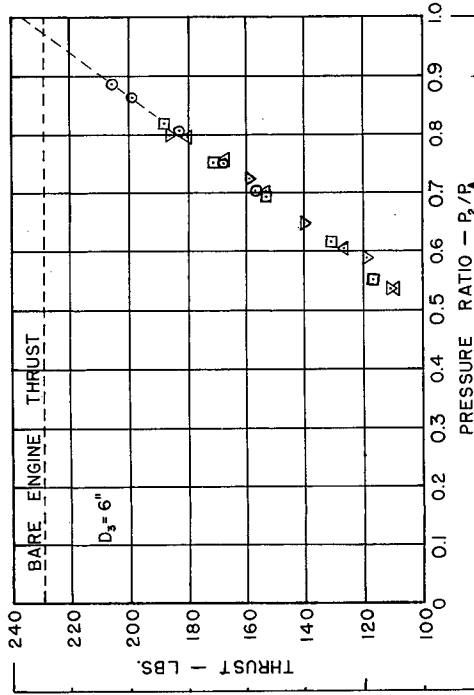


FIGURE 20  
THRUST vs. SECONDARY PRESSURE RATIO  
 $A_3/A_1 = 2.48$

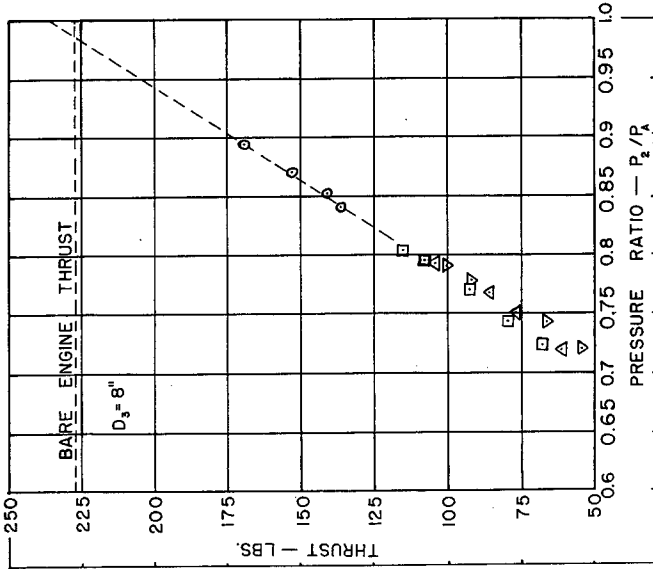


FIGURE 21  
THRUST vs. SECONDARY PRESSURE RATIO  
 $A_3/A_1 = 4.30$

SYMBOLS:

- $\circ$  - 2.5  $D_3 = L$
- $\square$  - 5.0  $D_3 = L$
- $\triangle$  - 7.5  $D_3 = L$
- $\nabla$  - 10.0  $D_3 = L$

$T_1/T_A = 3.32$   
 $P_1/P_A = 1.91$   
 $\ell = 0$

## THE EFFECT OF MIXING TUBE LENGTH ON EJECTOR THRUST

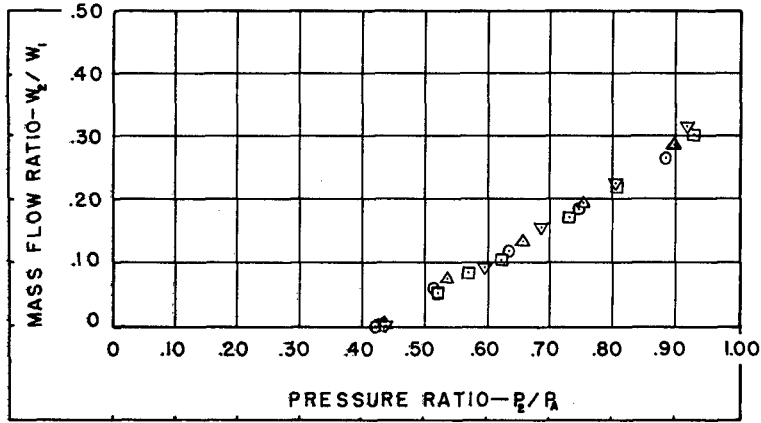


FIGURE 22

MASS FLOW RATIO vs. SECONDARY PRESSURE RATIO

**THE EFFECT OF  
PRIMARY TEMPERATURE VARIATION  
ON EJECTOR PERFORMANCE**

SYMBOLS:  $T_1/T_2$   
 $\circ = 2.09$        $R_1/P_1 = 1.91$   
 $\Delta = 2.52$        $A_2/A_1 = 1.72$   
 $\square = 3.32$        $L = 0$   
 $\nabla = 3.92$        $L = 7.5D_2$

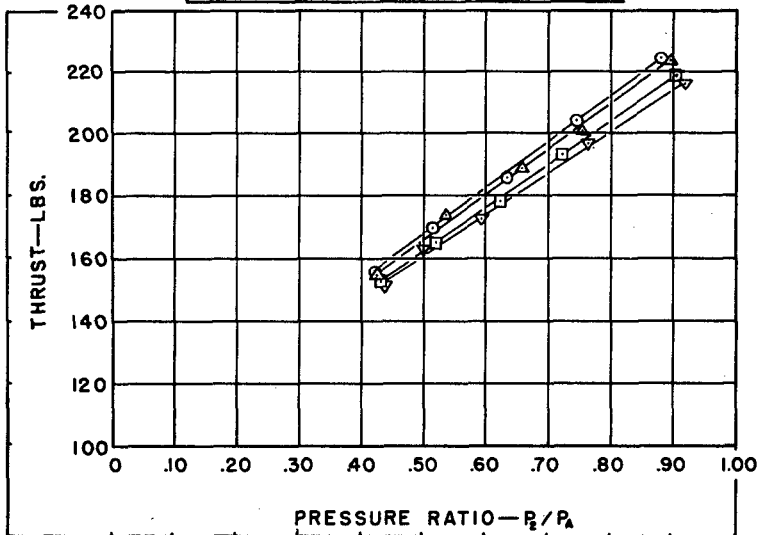


FIGURE 23

THRUST vs. SECONDARY PRESSURE RATIO

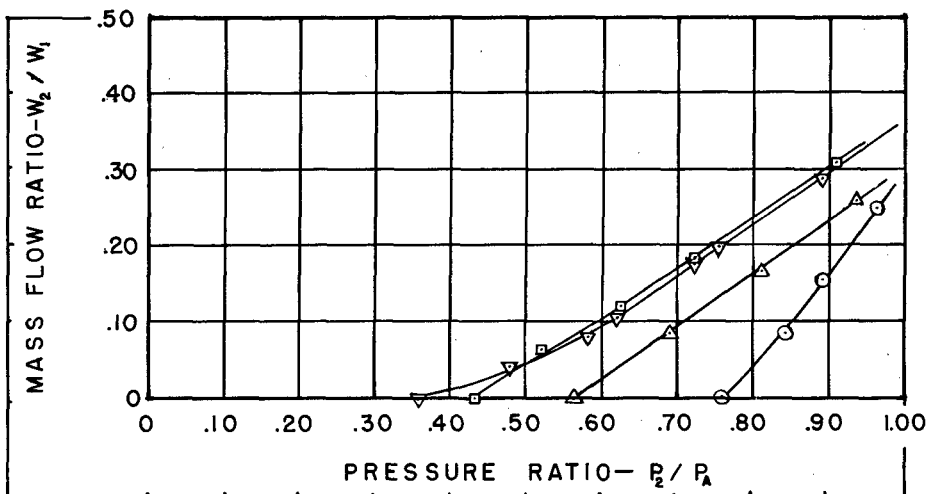


FIGURE 24

MASS FLOW RATIO vs. SECONDARY PRESSURE RATIO

### THE EFFECT OF PRIMARY PRESSURE VARIATION ON EJECTOR PERFORMANCE

SYMBOLS:  $P_1/P_A$   
 ○ = 1.35       $T_1/T_A = 3.32$   
 △ = 1.62       $A_3/A_1 = 1.72$   
 □ = 1.91       $\alpha = 0$   
 ▽ = 2.31       $L = 7.5 D_3$   
 - - - = BARE ENGINE THRUST

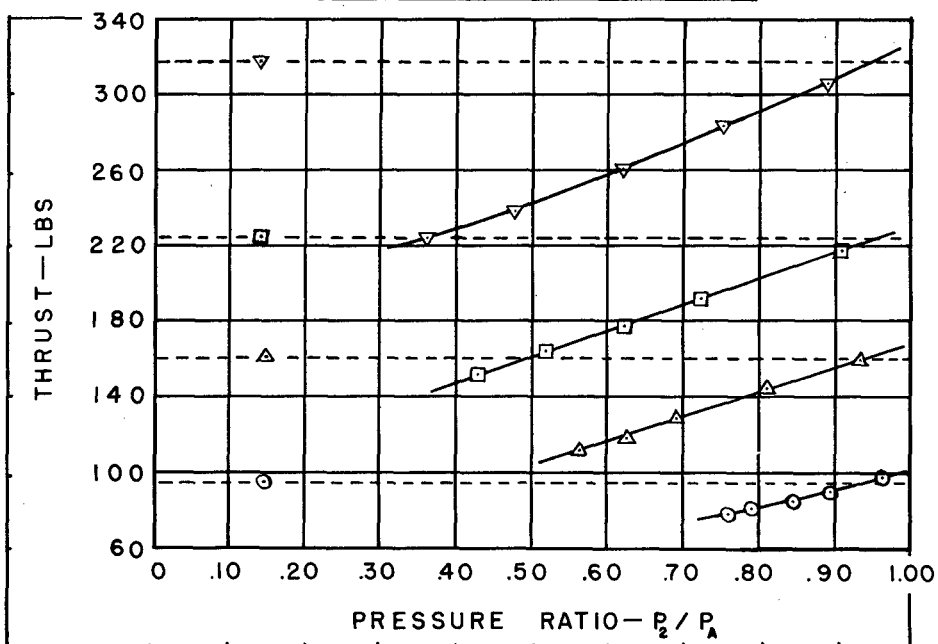
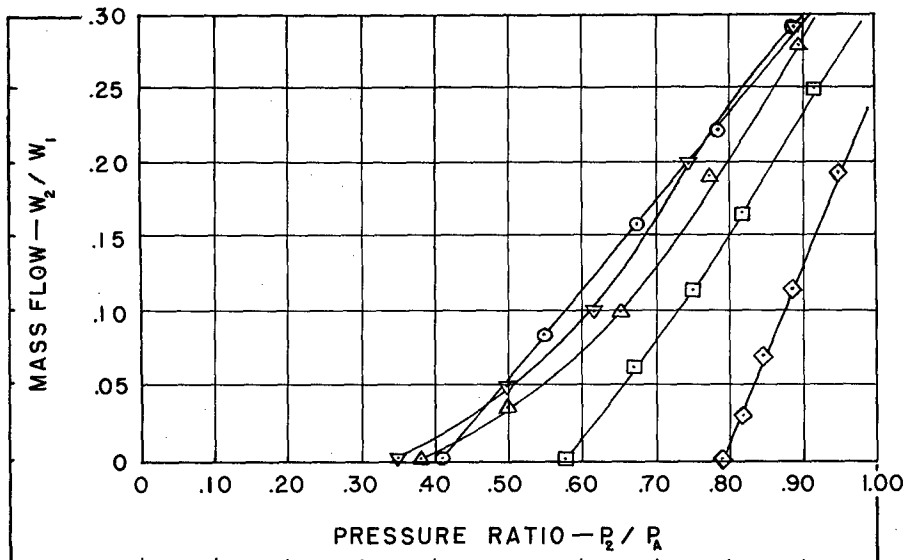


FIGURE 25

THRUST vs. SECONDARY PRESSURE RATIO



MASS FLOW RATIO vs. SECONDARY PRESSURE RATIO

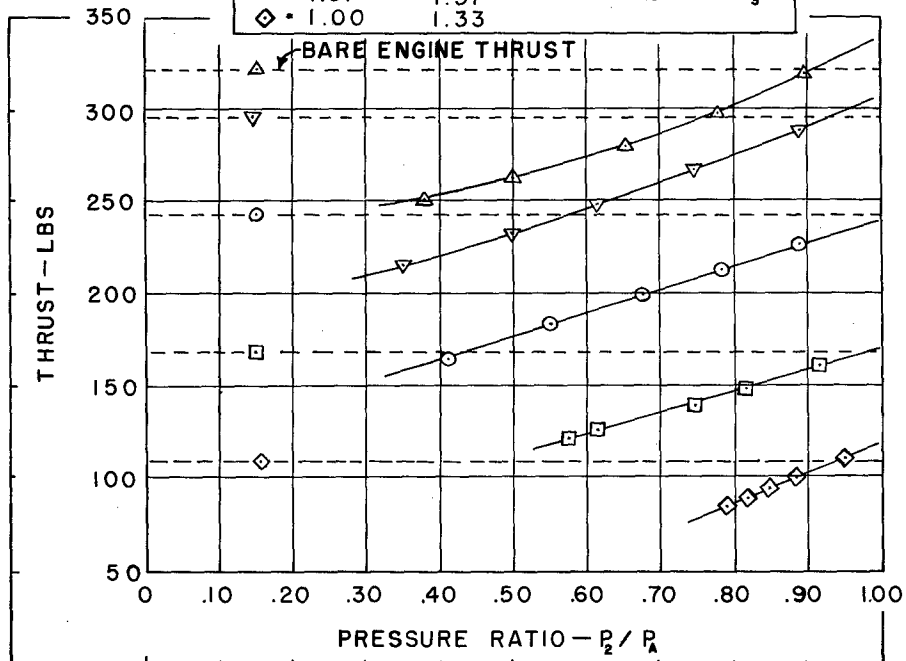
FIGURE 26

### EJECTOR PERFORMANCE

AT

### CONSTANT PRIMARY MASS FLOW

SYMBOLS:		
$T_1/T_A$	$P_1/P_A$	$W_1 = 4.81 \text{ lbs/sec.}$
$\Delta = 3.72$	2.38	$A_3/A_1 = 1.72$ $Q = 0$ $L = 7.5 D_3$
$\nabla = 3.32$	2.26	
$\circ = 2.52$	1.92	
$\square = 1.07$	1.57	
$\diamond = 1.00$	1.33	

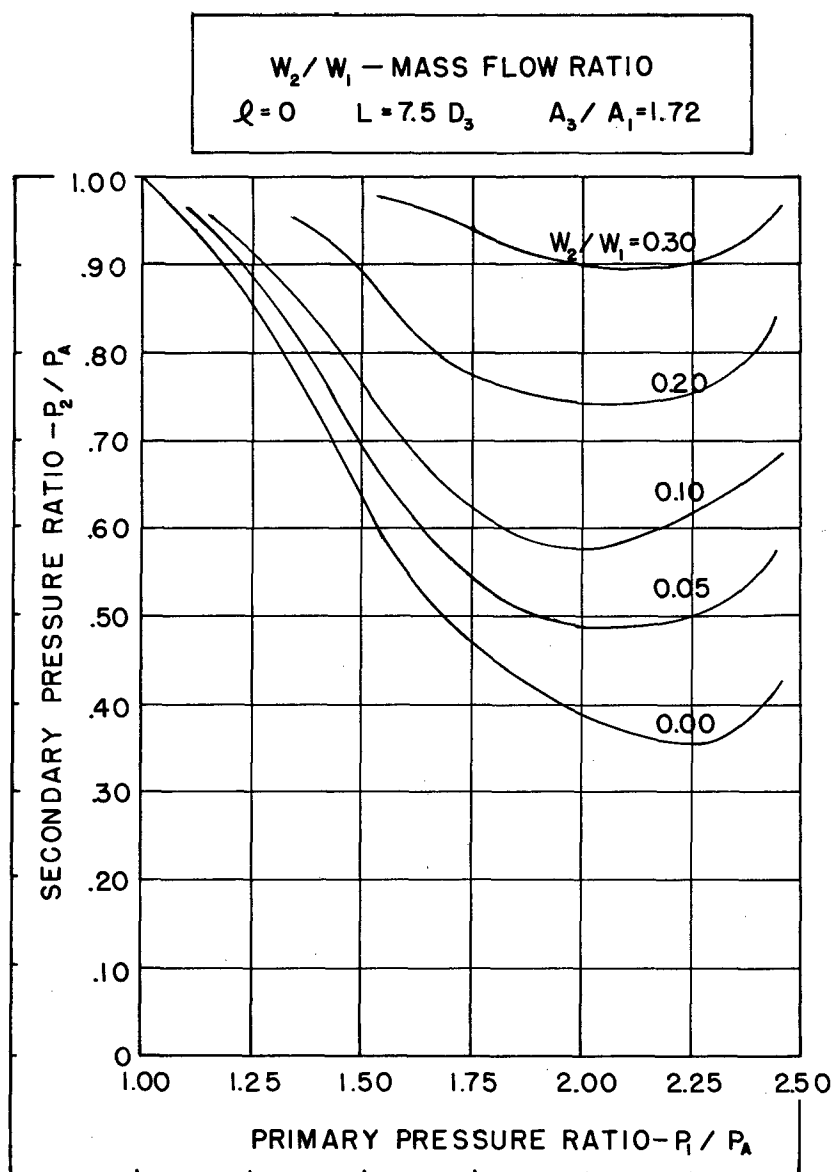


THRUST vs. SECONDARY PRESSURE RATIO

FIGURE 27

# DETERMINATION OF OPTIMUM PRIMARY PRESSURE RATIO

FIGURE 28



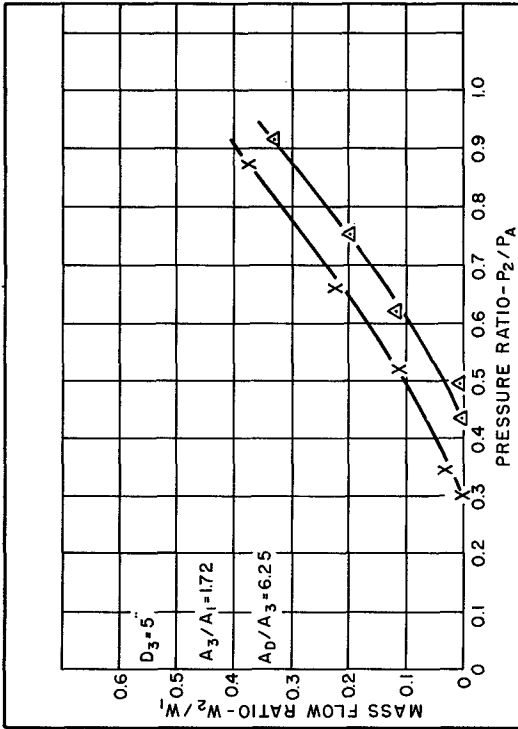


FIGURE 29  
MASS FLOW vs. SECONDARY PRESSURE RATIO

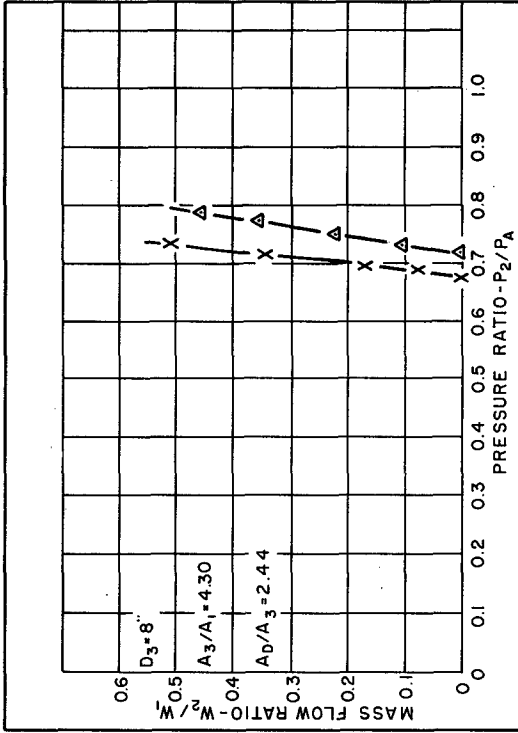


FIGURE 31  
MASS FLOW vs. SECONDARY PRESSURE RATIO

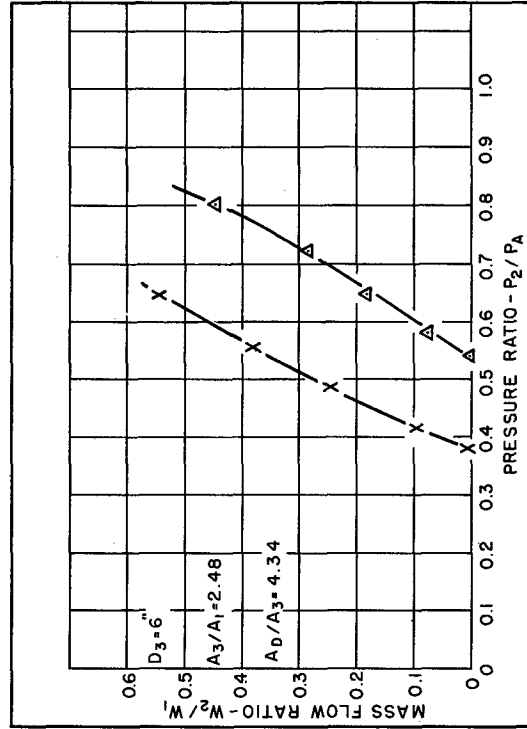
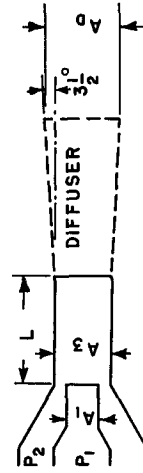


FIGURE 30  
MASS FLOW vs. SECONDARY PRESSURE RATIO



SYMBOLS:  
 Δ WITHOUT DIFFUSER  
 X WITH 7° DIFFUSER  
 $T_1/T_A = 3.32$   $\theta = 0$   
 $P_1/P_A = 1.91$   $L = 7.5D_3$

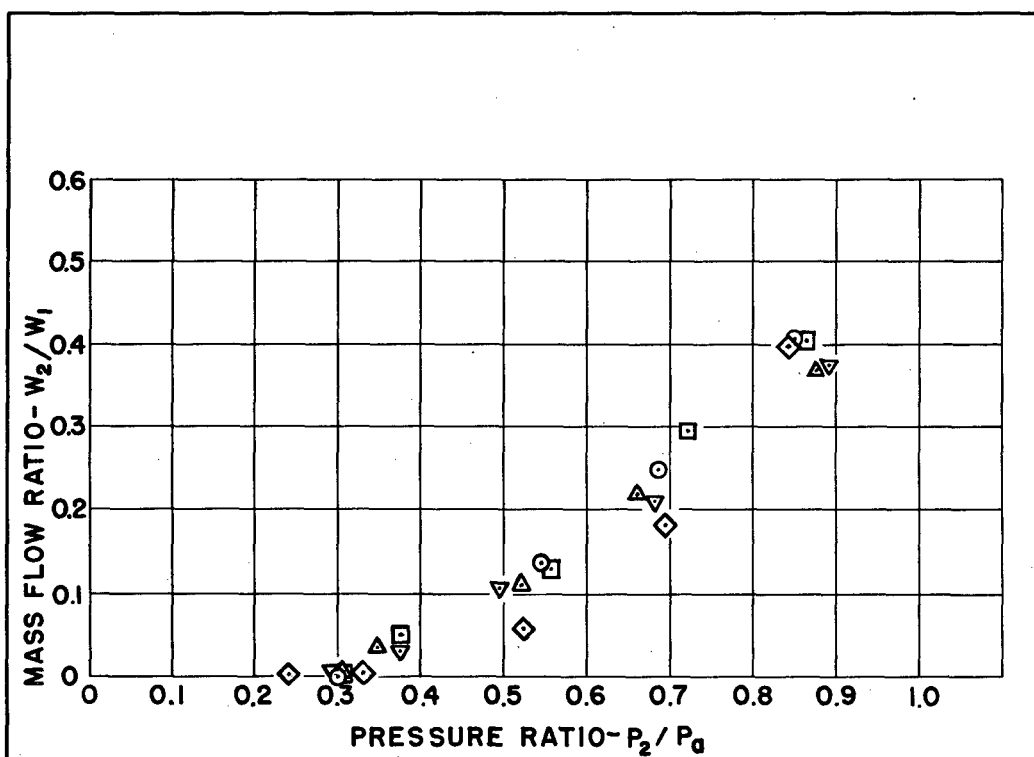
EFFECT OF DIFFUSER  
 ON  
 EJECTOR PERFORMANCE

# EFFECT OF DIFFUSER ON EJECTOR PERFORMANCE

(AT DIFFERENT MIXING TUBE LENGTHS)

FIGURE 32

SYMBOLS:	$T_1/T_A = 3.32$
$L = \diamond - 0D_3$	$A_3/A_1 = 1.72$
$L = \circ - 2.5D_3$	$D_3 = 5''$
$L = \square - 5.0D_3$	$P_1/P_0 = 1.91$
$L = \triangle - 7.5D_3$	$l = 0$
$L = \nabla - 10.0D_3$	$A_0/A_3 = 6.25$



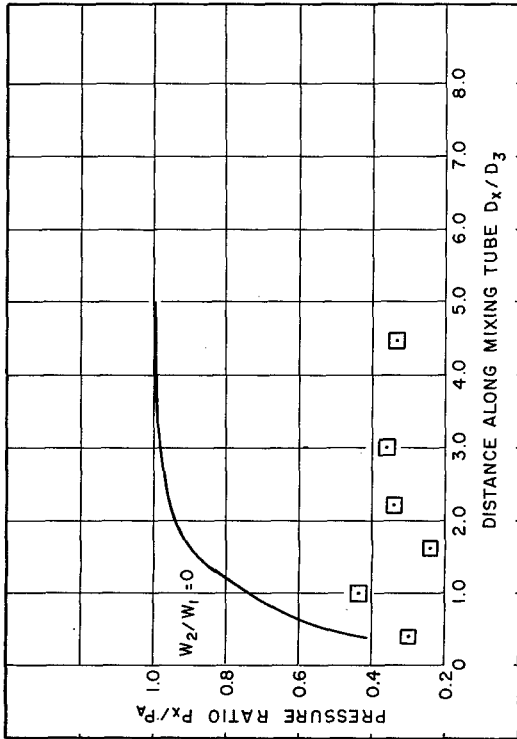


FIGURE 33  
STATIC PRESSURE RATIO ALONG MIXING TUBE

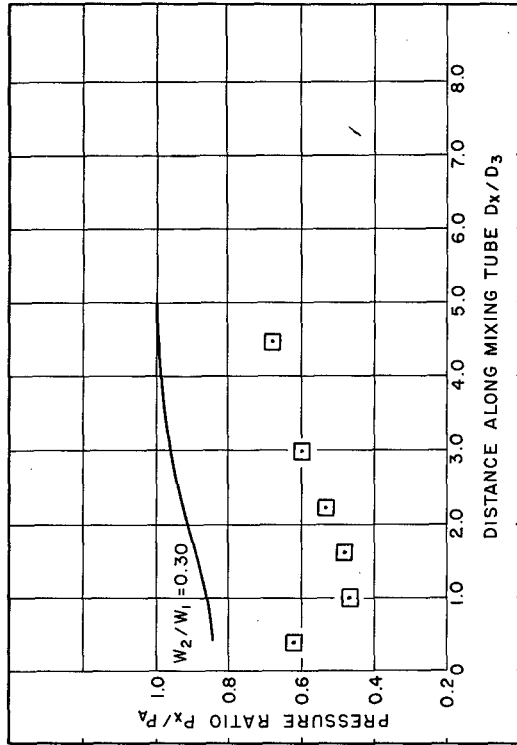


FIGURE 35  
STATIC PRESSURE RATIO ALONG MIXING TUBE

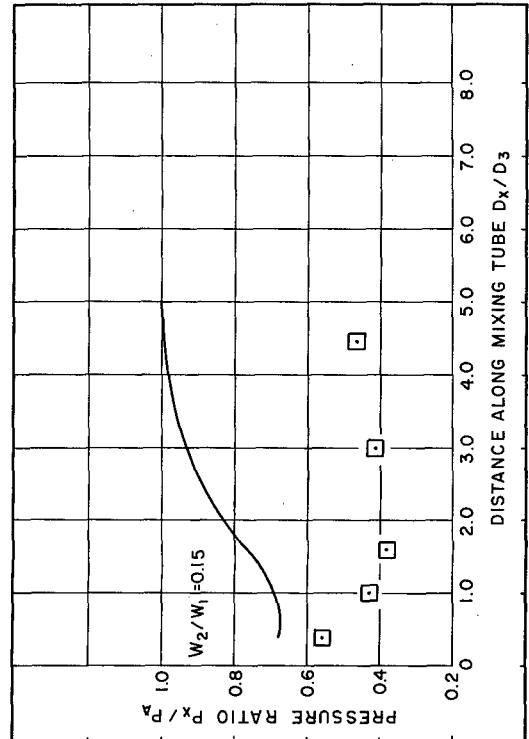


FIGURE 34  
STATIC PRESSURE RATIO ALONG MIXING TUBE

SYMBOLS:  
 — WITHOUT DIFFUSER  
 □ WITH DIFFUSER  
 $L = 5 D_3$        $\ell = 0$   
 $P_1/P_0 = 1.91$        $T_1/T_0 = 3.32$   
 $W_2/W_1$  - MASS FLOW RATIO

**STATIC PRESSURE DISTRIBUTION  
 ALONG  
 MIXING TUBE**  
 ( $A_3/A_1 = 1.72$ ,  $D_3 = 5''$ )

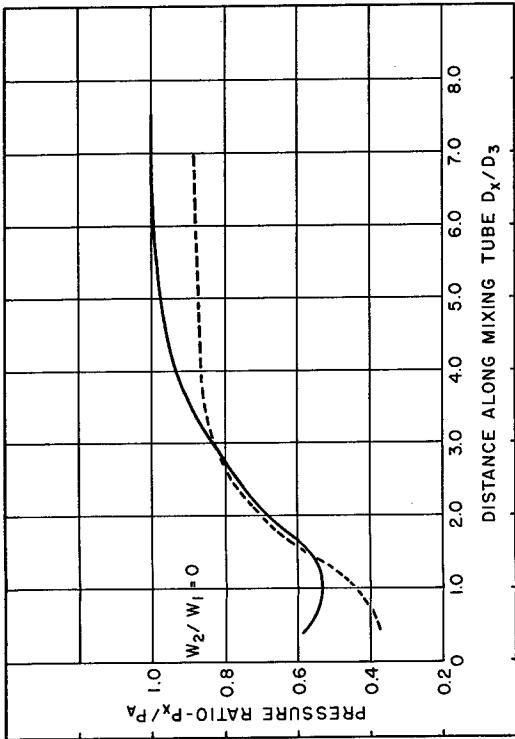


FIGURE 36  
STATIC PRESSURE RATIO ALONG MIXING TUBE

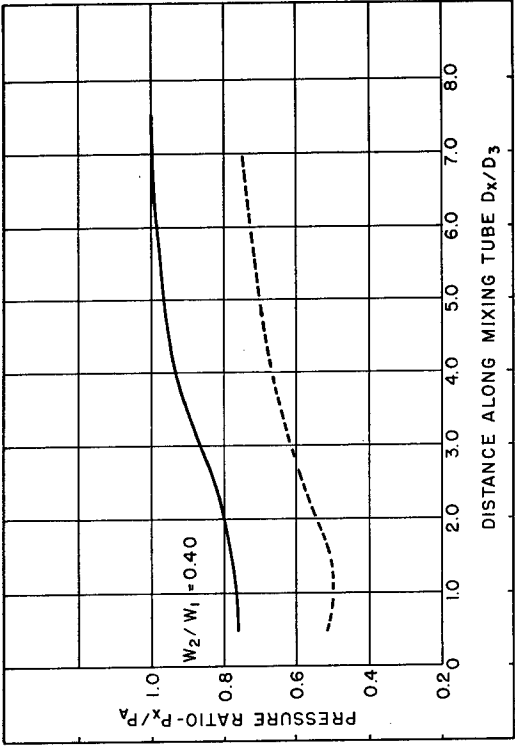


FIGURE 38  
STATIC PRESSURE RATIO ALONG MIXING TUBE

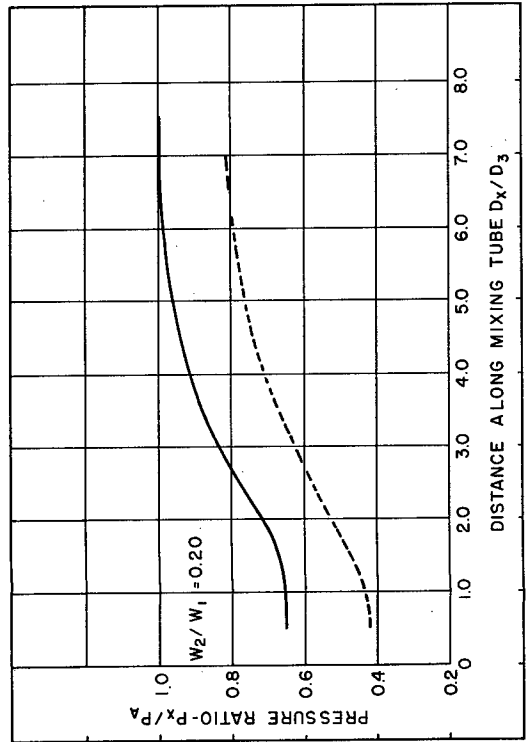


FIGURE 37  
STATIC PRESSURE RATIO ALONG MIXING TUBE

SYMBOLS:  
 — WITHOUT DIFFUSER  
 --- WITH 7° DIFFUSER  
 $L = 7.5D_3$      $\beta = 0$   
 $P_1/P_0 = 1.91$      $T_1/T_0 = 3.32$   
 $W_2/W_1$  - MASS FLOW RATIO

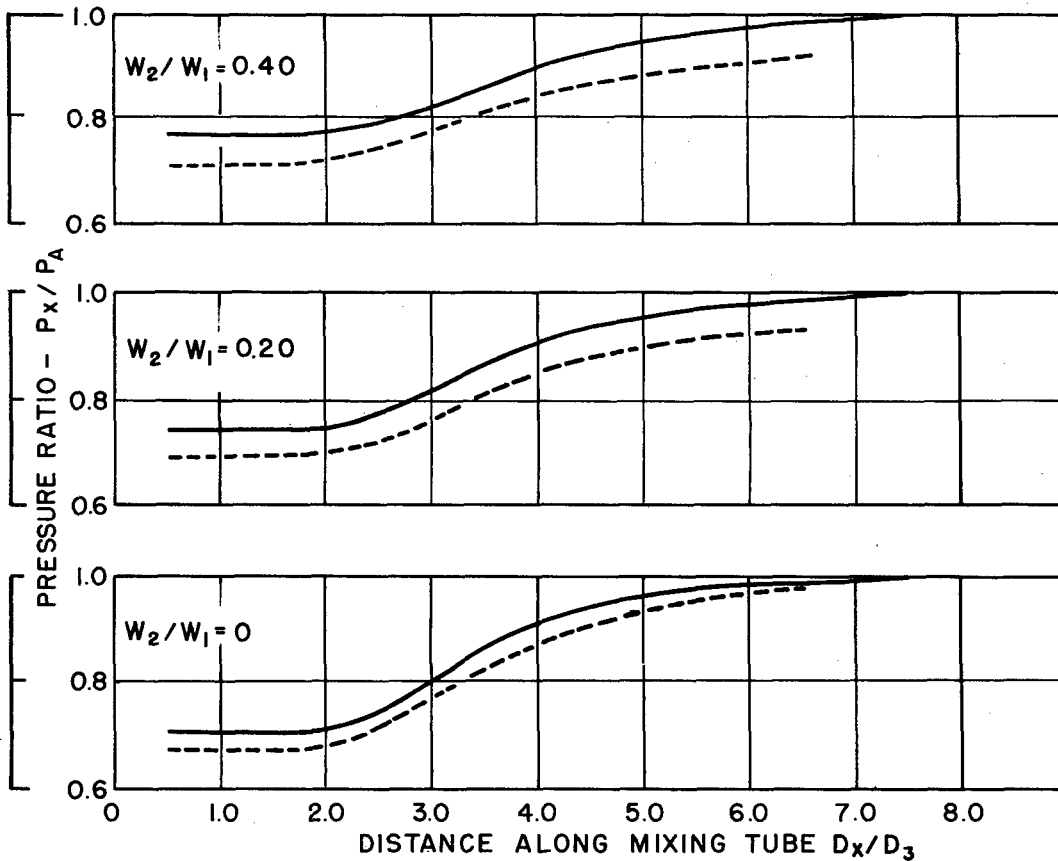
STATIC PRESSURE DISTRIBUTION  
 ALONG  
 MIXING TUBE  
 ( $A_3/A_1 = 2.48, D_3 = 6$ )

# STATIC PRESSURE DISTRIBUTION ALONG MIXING TUBE

( $A_3/A_1 = 4.30$      $D_3 = 8''$ )

FIGURE 39

**SYMBOLS:**  
 — WITHOUT DIFFUSER  
 --- WITH 7° DIFFUSER  
 $L = 7.5D_3$      $\ell = 0$   
 $P_1/P_A = 1.91$      $T_1/T_A = 3.32$   
 $W_2/W_1$  - MASS FLOW RATIO



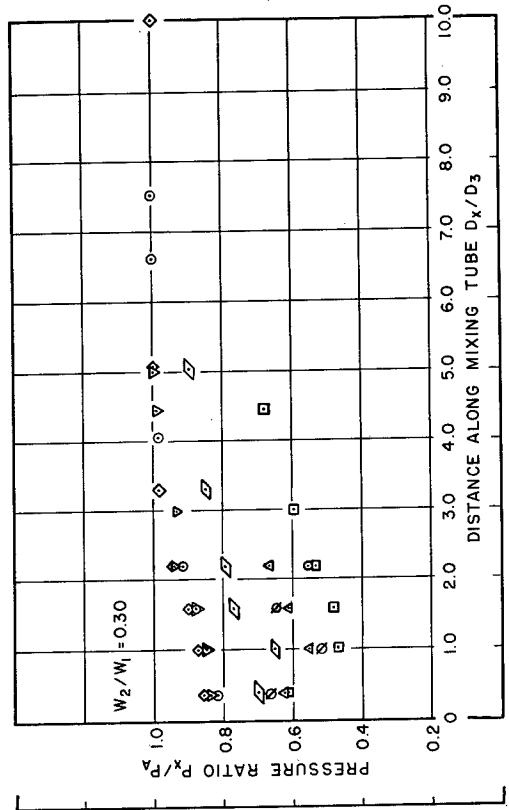


FIGURE 42  
STATIC PRESSURE RATIO ALONG MIXING TUBE

SYMBOLS:  
 L-WITH DIFF. WITHOUT DIFF.  
 2.5D<sub>3</sub> ▴ ▽  
 5.0D<sub>3</sub> □ ◻  
 7.5D<sub>3</sub> ⊗ ⊙  
 10.0D<sub>3</sub> ⊠ ⊡  
 A<sub>3</sub>/A<sub>1</sub> = 1.72 D<sub>3</sub> = 5" L = 7.5D<sub>3</sub>  
 P<sub>1</sub>/P<sub>0</sub> = 1.91 T<sub>1</sub>/T<sub>0</sub> = 3.32 ε = 0

STATIC PRESSURE DISTRIBUTION  
ALONG  
MIXING TUBE

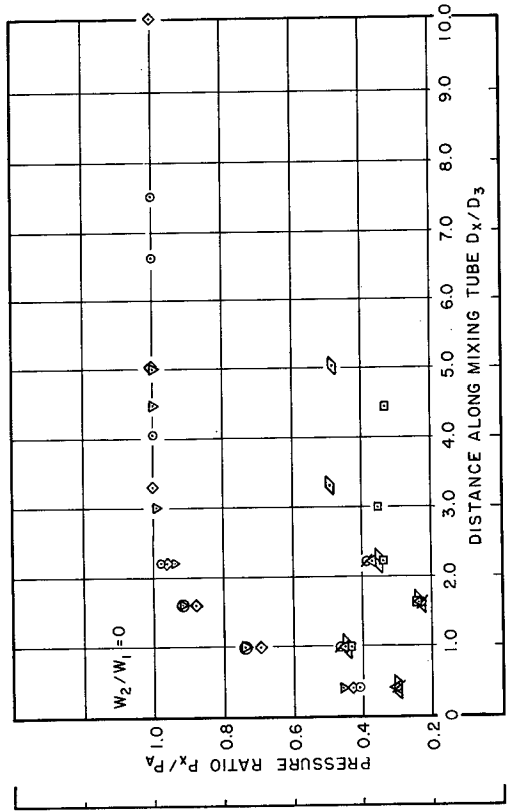


FIGURE 40  
STATIC PRESSURE RATIO ALONG MIXING TUBE

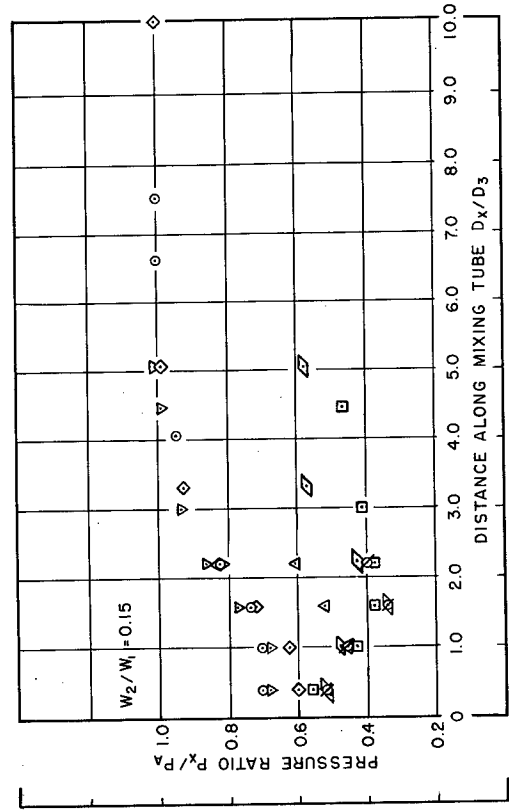
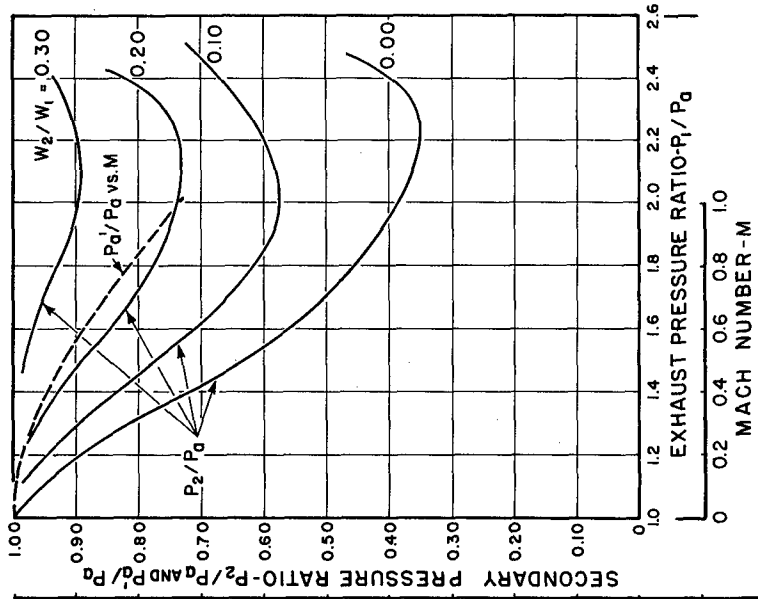


FIGURE 41  
STATIC PRESSURE RATIO ALONG MIXING TUBE

APPLICATION OF EJECTOR DATA TO  
AN AIRCRAFT INSTALLATION



EJECTOR  
CONDITIONS:  
 $A_3/A_1 = 1.72$   
 $\alpha = 0$   
 $L = 75D_3$   
 $T_1/T_0 = 3.32$   
 $W_2/W_1 =$  MASS FLOW RATIO  
 $P_d/P_0 =$  MINIMUM PRESSURE  
RATIO FOR NACA 66-(12),12  
AIRFOIL SECTION AT  $C_{*} = 0.20$

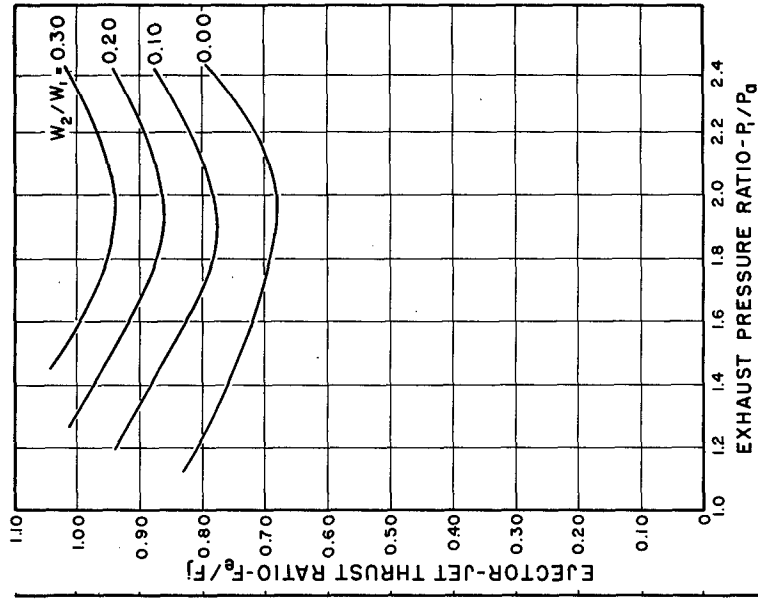


FIGURE 43  
PRESSURE RATIO REQUIRED  
AND AVAILABLE FOR EJECTOR  
BOUNDARY LAYER REMOVAL

FIGURE 44  
EJECTOR-JET THRUST RATIO  
FOR VARIOUS FLOW CONDITIONS